iScience

CellPress
OPEN ACCESS

Article

PI3K-dependent reprogramming of hexokinase isoforms controls glucose metabolism and functional responses of B lymphocytes

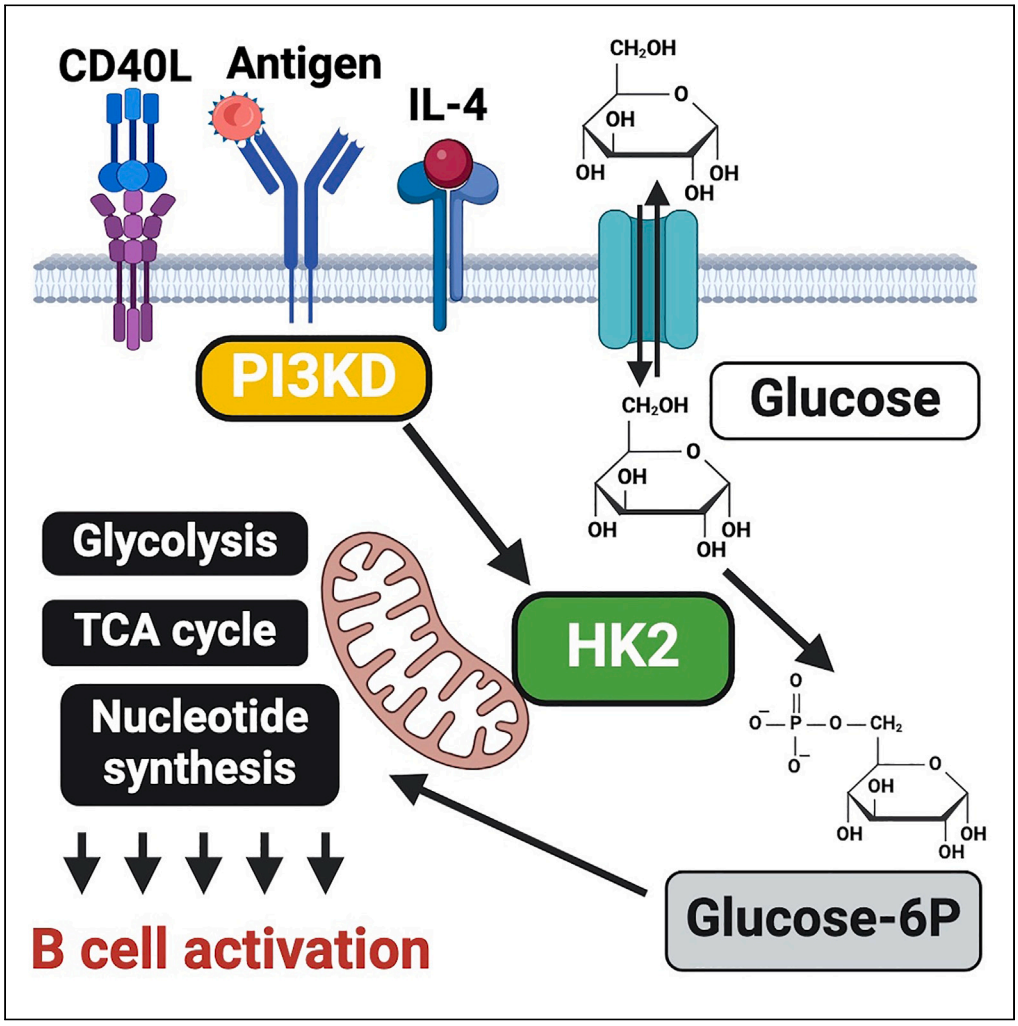

Brandon T. Paradoski, Sen Hou, Edgard M. Mejia, ..., Nissim Hay, Hu Zeng, Aaron J. Marshall

aaron.marshall@umanitoba.ca

Highlights

HK2 expression and mitochondrial localization in B cells are modulated by PI 3-kinase

HK2 deficiency impairs B cell metabolism and glucose utilization in multiple pathways

HK2 deficiency impairs B cell responses to stimulation, despite metabolic adaptation

HK2 is required for optimal germinal center, plasma cell, and antibody responses

Paradoski et al., iScience 27, 110939
October 18, 2024
https://doi.org/10.1016/j.isci.2024.110939

iScience

CellPress
OPEN ACCESS

Article

PI3K-dependent reprogramming of hexokinase isoforms controls glucose metabolism and functional responses of B lymphocytes

Brandon T. Paradoski,[1,10] Sen Hou,[1,10] Edgard M. Mejia,[1,10] Folayemi Olayinka-Adefemi,[1] Danielle Fowke,[1] Grant M. Hatch,[2,5] Ayesha Saleem,[5,6] Versha Banerji,[4,7] Nissim Hay,[8] Hu Zeng,[9] and Aaron J. Marshall[1,3,4,7,11,*]

SUMMARY

B lymphocyte activation triggers metabolic reprogramming essential for B cell differentiation and mounting a healthy immune response. Here, we investigate the regulation and function of glucose-phosphorylating enzyme hexokinase 2 (HK2) in B cells. We report that both activation-dependent expression and mitochondrial localization of HK2 are regulated by the phosphatidylinositol 3-kinase (PI3K) signaling pathway. B cell-specific deletion of HK2 in mice caused mild perturbations in B cell development. HK2-deficient B cells show impaired functional responses *in vitro* and adapt to become less dependent on glucose and more dependent on glutamine. HK2 deficiency impairs glycolysis, alters metabolite profiles, and alters flux of labeled glucose carbons into downstream pathways. Upon immunization, HK2-deficient mice exhibit impaired germinal center, plasmablast, and antibody responses. HK2 expression in primary human chronic lymphocytic leukemia (CLL) cells was associated with recent proliferation and could be reduced by PI3K inhibition. Our study implicates PI3K-dependent modulation of HK2 in B cell metabolic reprogramming.

INTRODUCTION

The reprogramming of cellular metabolism to adapt to high rates of proliferation within different tissue environments is a concept well established in the context of cancer and more recently in the context of immune responses. The metabolic process of breaking down glucose into lactic acid even in the presence of ubiquitous oxygen to provide energy for cancerous cells was named "Aerobic Fermentation" by Warburg[1] and is known today as the "Warburg Effect." During an immune response, lymphocytes undergo dramatic remodeling of their cellular metabolic pathways in order to meet the demands of rapid cell proliferation and new effector functions. However, activated lymphocyte subsets exhibit variable dependence on glucose and other metabolic fuels to provide both energy and the building blocks needed for the biosynthesis of nucleic acids and glycoproteins such as antibodies.

Upon activation with antigen and costimulatory signals, B cells must rapidly transition from a quiescent state to a highly active state of rapid cell division, which requires profound metabolic reprogramming. B cells reprogram their metabolism by selecting the appropriate metabolic pathways to generate energy as well as the needed biomolecules to progress through cell growth, division, differentiation, and effector function.[2–4] Resting B cells consume low amounts of macromolecules to provide energy for their basal metabolic processes and perform little glycolysis. Mitochondrial oxidative phosphorylation appears to be important for energy production, as resting B cells are sensitive to the inhibition of ATP synthase using the inhibitor oligomycin and have been suggested to predominantly break down fatty acids via the process of β-oxidation. Resting B cells are maintained in their quiescent state by glycogen synthase kinase 3 (GSK3), which prevents cell growth and proliferation, preserves redox levels, and inhibits glycolysis to allow for long-lived B cell quiescence.[5]

Upon activation, B cells switch to an anabolic state where ATP is more rapidly produced and utilized in building macromolecules such as proteins, nucleotides, and lipids to allow for cell growth, DNA synthesis, and cell division.[6,7] This is largely achieved by the transcription factor

[1]Departments of Immunology, University of Manitoba, Winnipeg, Canada
[2]Pharmacology and Therapeutics, University of Manitoba, Winnipeg, Canada
[3]Biochemistry and Medical Genetics, University of Manitoba, Winnipeg, Canada
[4]Internal Medicine, Rady Faculty of Health Sciences, University of Manitoba, Winnipeg, Canada
[5]The Children's Hospital Research Institute of Manitoba, Winnipeg, Canada
[6]Faculty of Kinesiology and Recreation Management, University of Manitoba, Winnipeg, Canada
[7]Paul Albrechtsen Research Institute, Cancer Care Manitoba, Winnipeg, Canada
[8]Department of Biochemistry and Molecular Genetics, University of Illinois, Chicago, IL, USA
[9]Department of Immunology and Division of Rheumatology, Mayo Clinic, Rochester, MN, USA
[10]These authors contributed equally
[11]Lead contact
*Correspondence: aaron.marshall@umanitoba.ca
https://doi.org/10.1016/j.isci.2024.110939

cMyc and the kinase mTORC1, which drive new transcription and protein translation, respectively, to reprogram B cell metabolism,[3] including a rise in glucose transporter expression and a 10-fold increase in glucose uptake.[4] Phosphatidylinositol (PI) 3-kinases (PI3Ks) initiate a critical signaling cascade acting via PI-binding proteins such as Akt, PDK1, and TAPP1/2 to control cMyc and mTOR activity and increase glucose utilization.[7,8] B cell activation via the antigen receptor alone causes B cells to initiate glycolysis and oxidative phosphorylation to support anabolic increase in cell size. Co-engagement of the inhibitory receptor FcγRIIB reduces glucose uptake and glycolysis.[6] Antigen receptor activation without a second signal from a T cell (e.g., CD40L + IL-4) or innate immune receptor (TLR9) leads to mitochondrial swelling, increased reactive oxygen species levels, and dysregulated Ca^{2+} signaling, ultimately resulting in activation-induced cell death.[9] Activation via CD40L + IL-4 was found to divert glucose into the pentose phosphate pathway for nucleotides and NADPH synthesis as well as fatty acid and cholesterol synthesis needed for cellular membrane production and cell division.[6,9,10] Taken together, the specific metabolic pathways used by acutely activated B cells are time- and signal dependent, which coincides with the cellular changes necessary to proliferate and carry out immune functions.

Metabolic heterogeneity among different B cell subsets is not entirely understood. Anergic B cells exhibit reduced PI3K pathway activity, are metabolically quiescent, and show reduced ability to produce antibodies, while chronic activation of B cells via BAFF led to enhanced metabolism, which correlated with sustained PI3K pathway activity.[11,12] Selection of high-affinity antigen-specific B cells during the germinal center (GC) response requires continuous cycles of cell division and affinity selection for many weeks, within a distinct hypoxic micro-environment.[13,14] We and others have found that GC B cells (GCBs) express more GLUT1 on their cell surface and have a higher glucose uptake rate than naive follicular B cells.[5,8] GCBs receiving positive selective signals upregulate cMyc and require mTOR-dependent anabolic metabolism to undergo subsequent proliferation.[15–17] Upon differentiation into effector plasma cells (PCs), B cells undergo a further metabolic transformation, devoting tremendous resources to protein synthesis and glycosylation required for high-rate antibody production.[18,19] PCs take up large amounts of glucose to support energy production and synthesis of glycosylated antibodies.[18,20] Thus, GC and PC populations appear highly dependent on glucose metabolism.

Glucose enters activated B cells though glucose transporters (primarily GLUT1, 3, and 4) and is phosphorylated at the carbon six position by one of the four hexokinase (HK) enzymes to form glucose-6-phosphate (G6P).[21] G6P can then be utilized by one of several important metabolic pathways such as glycolysis, oxidative phosphorylation, the pentose phosphate pathway (PPP), or the hexosamine biosynthetic pathway. Using ^{13}C-glucose tracing, glucose-derived carbons can also be found interconverted into lipids, amino acids, and other sugars.[2] While mitochondrial oxidative phosphorylation has an advantage over cytosolic glycolysis in energy production, it also consumes potential sources of biosynthetic precursors and generates reactive oxygen species that can reach toxic levels. Thus, these processes must be carefully balanced within rapidly proliferating cells. Targeting glucose metabolism with drugs such as 2-deoxyglucose (2DG) significantly suppressed B cell proliferation and antibody production, while B cell-specific deletion of GLUT1 resulted in impaired B cell numbers or antibody production.[11]

The phosphoinositide 3-kinase (PI3K) signaling pathway is activated by antigen and costimulatory receptors and plays a central role in B cell metabolic reprograming.[3,21,22] We and others have reported that increased glucose uptake upon B cell activation is partly dependent on the PI3K pathway[5,6,8]; however, our understanding of the underlying mechanisms remains rudimentary. PI3Ks function by phosphorylating plasma membrane lipids to generate D3 phosphoinositides, which regulate the activity of over 100 PI-binding proteins,[23–25] including the extensively studied serine-threonine kinase Akt. Akt can phosphorylate and inactivate GSK3 to prevent its functions in maintaining B cell quiescence,[5] and regulate mTOR via phosphorylation and inactivation of mTOR inhibitors PRAS40 and TSC2.[26,27] Akt1/2-deficient B cells show impaired cMyc expression and mTOR activity, reduced glucose uptake and cell growth, and mount poor GC and PC responses.[28] We found that uncoupling of TAPP1/2 from the PI3K product PI(3,4)P2 leads to hyperactivation of Akt, increased glucose uptake, and B cell hyperactivation *in vitro* and *in vivo*.[8] We and others have shown that PI3K can regulate the expression of glucose transporter GLUT1,[8,11,29–31] suggesting that one mechanism by which PI3K promotes glucose utilization is by ensuring sufficient glucose transport capacity.

While GLUTs are bidirectional transporters facilitating diffusion across the membrane, the intracellular retention and utilization of glucose requires the action of HKs. HKs are enzymes that phosphorylate glucose to G6P, which maintains the concentration gradient for glucose to continue entering into the cell while retaining G6P intracellularly.[32] G6P can be diverted into several distinct metabolic pathways, including glycolysis, conversion into glycogen for the storage of energy, entry into the PPP for NADPH and nucleotide production, or entry into the hexosamine biosynthesis pathway to glycosylate proteins.[33] There are four HK protein isoforms that differ in their respective enzyme kinetics, subcellular localization, and tissue expression.[33,34] While HK1 is ubiquitously expressed, other isoforms show restricted expression patterns. The HK2 isoform is expressed at very low levels in resting T lymphocytes, but is sharply elevated upon activation[35]; the expression pattern of HK isoforms in B lymphocytes has not been determined. Regulated localization of HK1 to mitochondria vs. cytoplasm was recently found to impact the metabolic fate of glucose and cellular functions of macrophages.[36] In non-immune cells, HK2 can shuttle between mitochondria and cytoplasm in a regulated manner[37]; however its subcellular localization in B lymphocytes remains to be determined.

Here, we examined whether reprogramming of HK isoforms occurs during B cell activation, uncovering a marked upregulation of HK2 and regulated mitochondrial localization during B cell activation that both depend in part on the PI3K/mTOR pathway. We further found that HK2 has unique roles in B cell development and activation as well as the generation of optimal antibody responses *in vivo*. Finally, we examine the role of HK2 in B cell metabolic reprogramming during activation, providing evidence that HK2 can impact glucose utilization in glycolysis as well as direct alternate metabolic fates of glucose. Together, our results strongly implicate HK2 upregulation as an important component of B cell metabolic reprogramming required for optimal glucose utilization and generation of humoral immune responses.

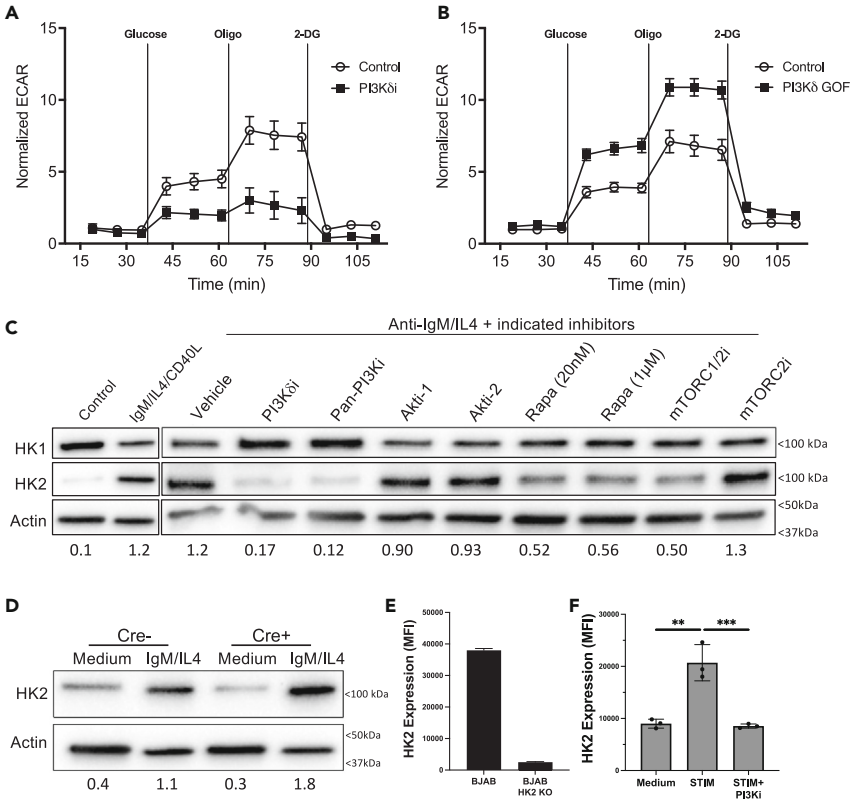

Figure 1. PI3K-dependent reprogramming of hexokinases during B cell activation

(A) Splenic B cells from C57BL/6 mice were stimulated overnight with anti-CD40+IL-4+anti-IgM with or without PI3Kδ inhibitor idelalisib (PI3Kδi), and extracellular acidification rate (ECAR) profile was assessed by Seahorse metabolic flux assay. The graph shows the mean and SEM of 5 technical replicates from one representative experiment (four performed).

(B) Splenic B cells isolated from mice with a B cell-specific PI3Kδ gain-of-function mutation (PI3Kδ GOF), or littermate control mice, were stimulated overnight with anti-CD40+IL-4+anti-IgM and ECAR profile was assessed. The graph shows the mean and SEM of 5 technical replicates from one representative experiment (three performed).

(C) Protein extracts were collected from resting or activated B cells, and the expression of HK1 or HK2 was detected by western blot. Impact of PI3K, Akt, and mTOR inhibitors on activation-induced HK1/2 expression was determined by the addition of inhibitors: PI3Kδi = 10 μM idelalisib; pan-PI3Ki = 1 μM pictilisib; Akti-1 = 1 μM MK-2206; Akti-2 = 1 μM iapatasertib; Rapa, rapamycin; mTORC1/2i = 50 nM sapanisertib; mTORC2i = 50 nM JR-AB2-011. Data are representative of two similar experiments with all inhibitors, and five others with PI3K inhibitors only. Numbers below each lane indicate the relative HK2/actin ratios.

(D) PI3Kδ GOF splenic B cells were stimulated overnight with anti-CD40+IL-4+anti-IgM prior to western blot analysis to detect HK2 expression levels. Data are representative of two similar experiments.

(E) Flow cytometry detection of HK2 upregulation in human B cells was validated by comparing BJAB human B lymphoma cells and BJAB cells where the HK2 gene was deleted by CRISPR. Data are representative of two similar experiments.

(F) Peripheral blood mononuclear cells (PBMCs) were stimulated overnight with CD40L + IL-4+anti-IgM with or without 1 μM pictilisib and then surface stained for CD19 and intracellularly stained for HK2. HK2 staining mean fluorescence intensity (MFI) among live $CD19^{+}$ cells is shown for cultures from 3 healthy donor PBMC samples. Results are pooled from two independent experiments.

RESULTS

Activation-induced reprograming of hexokinase isoforms is regulated by phosphoinositide 3-kinase delta

Previous studies have shown that inhibition of phosphoinositide 3-kinase (PI3K) activity results in decreased glycolysis in different cell types; however, its role in reprogramming glucose utilization during B cell activation is not completely understood. We examined the impact of idelalisib, a specific inhibitor of the delta isoform of PI3K (PI3Kδi), on extracellular acidification rate (ECAR), an indirect measure of glycolysis. Primary B cells were activated overnight, with or without PI3Kδi treatment, and their resulting ECAR was measured. Our results show that PI3Kδi treatment results in a significant decrease in glycolysis as well as glycolytic reserve, while basal ECAR was not affected (Figure 1A). Reciprocally, primary mouse B cells expressing PI3Kδ with a gain-of-function (GOF) mutation[38] showed markedly increased ECAR upon glucose addition (Figure 1B), indicating that hyperactive PI3Kδ can drive elevated glycolysis. Following uptake by glucose transporters, glucose phosphorylation by hexokinases (HKs) is a key step required to retain and utilize intracellular glucose after transport. We found that resting splenic B cells predominantly express HK1, with HK2 being expressed at very low levels; however, upon overnight stimulation, protein expression of

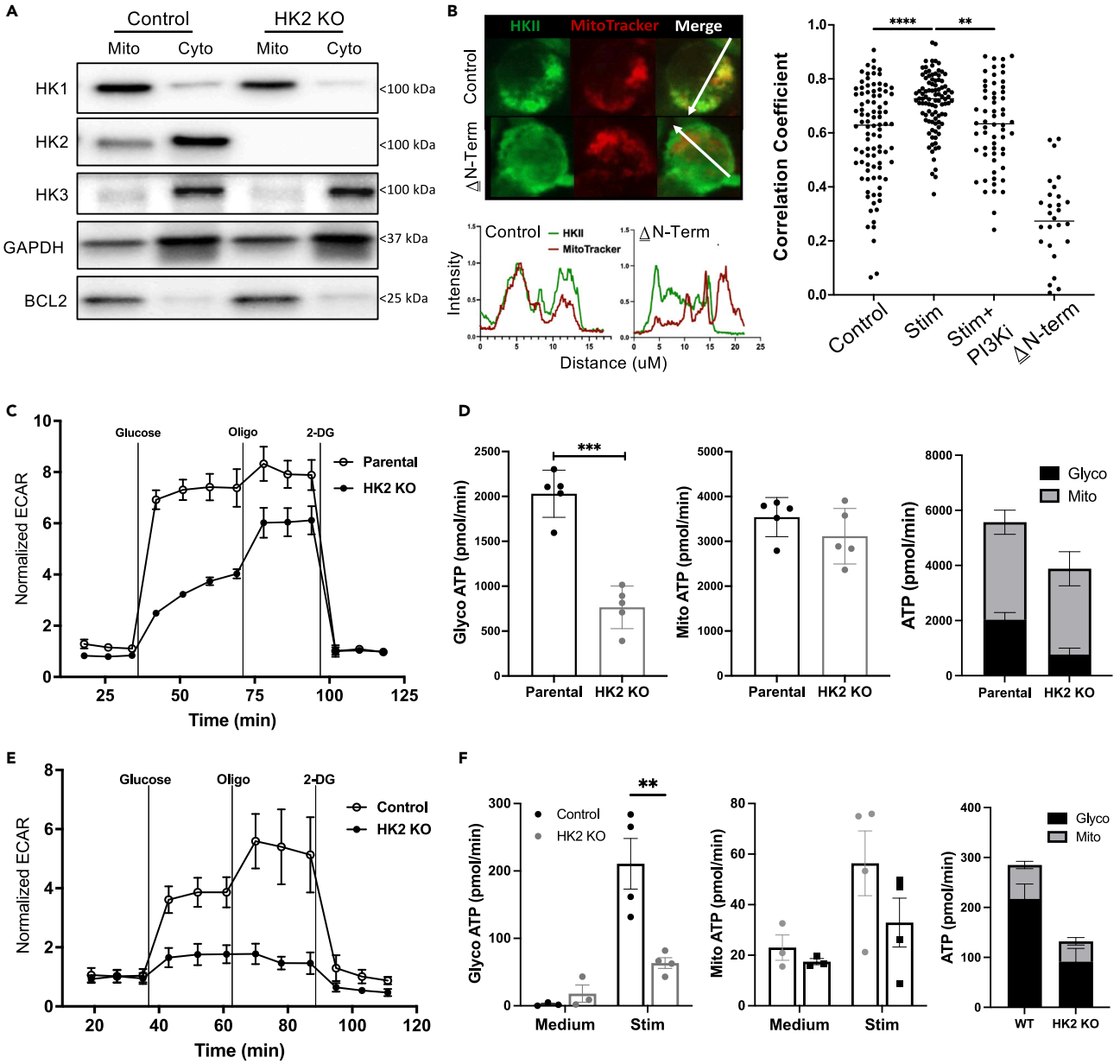

Figure 2. Unique subcellular localization and non-redundant function of HK2 in B cells

(A) Mitochondrial and cytoplasmic protein extracts were prepared from parental BJAB B lymphoma cells or HK2-deficient BJAB cells generated by Crispr gene inactivation. Extract were western blotted for HK1, 2, and 3; GAPDH was used as a positive control for cytoplasmic fraction enrichment while Bcl2 was used as a positive control for mitochondrial fraction enrichment. Data are representative of three similar experiments.

(B) Mitochondrial localization of HK2 in BJAB cells under various conditions was assessed by immunofluorescence staining of HK2, labeling of mitochondria with MitoTracker dye, and confocal microscopy analysis. HK2 KO BJAB cells re-expressing HK2 lacking the N-terminal mitochondrial localization sequence (ΔN-term) were used as a control. Left: representative images of cells expressing wild-type HK2 or ΔN-term, with green and red fluorescence intensity plots along the white arrows illustrating stronger colocalization for control versus mutant. Right: cells were assessed under low glucose conditions (Control), after treatment with anti-CD40+IL-4+anti-IgM (Stim) or pre-treatment with pictilisib prior to stimulation (Stim+PI3Ki). Graph depicts Pearson's correlation coefficients of HK2 and mitotracker staining signals for individual cells; results shown are pooled from two experiments showing similar results.

(C) Parental and HK2-deficient BJAB cells were assessed by metabolic flux assays and show significantly reduced ECAR. The graph shows the mean and SEM of 5 technical replicates from one representative experiment (two performed).

(D) Metabolic flux assay results indicating that HK2-deficient BJAB cells have significantly reduced glycolytic ATP production rate. The graph shows the mean and SEM of 5 technical replicates from one representative experiment (four performed).

Figure 2. *Continued*
(E and F) Splenic B cells were isolated from HK2-deficient or littermate control mice and cultured overnight in medium or anti-CD40, IL-4 and anti-IgM (Stim). Glycolysis was assessed by metabolic flux assays to measure ECAR in stimulated cells (E) or glycolytic/mitochondrial ATP production rates (F). ECAR and ATP assay results are each representative of two independent experiments.

HK2 was robustly increased while HK1 protein levels were unexpectedly found to decrease (Figure 1C). Interestingly, pre-treating cells with inhibitors of either PI3Kδ or all PI3K isoforms reversed this activation-dependent reprogramming of HK isoforms (Figure 1C). We further examined the role of two downstream targets of PI3K, Akt or mTOR, and found that inhibition of mTOR complex 1 using rapamycin or both mTOR complexes 1 and 2 using sapanisertib partially blocked HK2 upregulation, whereas inhibition of Akt or mTORC2 had little effect (Figure 1C). Conversely, B cells from PI3Kδ gain-of-function mutant mice showed a larger increase in HK2 expression after stimulation (Figure 1D). Expression of HK2 in human B cells was assessed using intracellular flow cytometry analysis, with specificity of staining validated in CRISPR knockout B lymphoma cells (Figure 1E). Primary human B cells also exhibited an increase in HK2 expression after activation, which was reversed by PI3K inhibition (Figure 1F). Taken together, these results indicate that B cell activation leads to PI3K-dependent increases in HK2 protein levels.

HK2 exhibits distinctive subcellular localization and PI3K-regulated association with mitochondria

In addition to expression levels, the localization of HK enzymes to the mitochondria is an important factor impacting their metabolic functions. To assess mitochondrial versus cytoplasmic localization of HK isoforms in lymphocytes, we utilized a human B lymphoma cell line BJAB that abundantly expresses HK1, 2, and 3. Western blot analysis of mitochondrial and cytoplasmic fractions revealed that HK1 is almost exclusively found in mitochondrial fractions, HK2 is split between mitochondrial and cytoplasmic fractions and HK3 is primarily found in cytoplasmic fractions (Figure 2A). We used confocal microscopy to further assess the impact of B cell activation and PI3K signaling on HK2 localization to mitochondria. Our results indicated that, under low glucose conditions, B cell activation increased HK2 localization to the mitochondria in a PI3K-dependent manner (Figure 2B). Together, these results confirm differential subcellular localization of HK isoforms in B cells and suggest that PI3K signaling may also regulate the subcellular localization of HK2 in the context of human B lymphoma cells.

HK2 has a non-redundant function in maximizing glycolysis

To determine whether HK2 has a non-redundant functional role in B cell metabolism, we used CRISPR to inactivate the HK2 gene in BJAB cells. We found that the absence of HK2 protein did not affect the expression or subcellular localization of HK1 or HK3 (Figure 2A). Assessment of ECAR revealed that the absence of HK2 results in a significant reduction in glycolysis (Figure 2C). Interestingly, parental BJAB B lymphoma cells show a minimal increase in ECAR upon inhibition of oxidative phosphorylation by oligomycin, indicating that high HK2 expression is associated with high constitutive glycolytic activity and minimal glycolytic reserve, while HK2-deficient cells are able to significantly increase their ECAR levels with the addition of oligomycin (Figure 2C). Analysis of ATP production rate revealed that HK2-deficient cells have impaired glycolytic ATP production rate, whereas mitochondrial ATP production rate was not significantly affected (Figure 2D). We further examined glycolysis in HK2-deficient primary mouse B cells after overnight activation *in vitro*. A significant reduction in ECAR after the addition of glucose was observed in HK2-deleted B cells compared to littermate controls (Figure 2E). In contrast to human B lymphoma cells, HK2-deleted mouse B cells appear to have diminished glycolytic reserve. Assessment of glycolytic and mitochondrial ATP production in HK2-deleted mouse B cells also indicated a specific impairment in energy production from glycolysis (Figure 2F). These results suggest that HK2 has non-redundant functions to maximize glycolysis in activated B cells, but is not essential for mitochondrial ATP production.

Impact of HK2 deficiency on B cell development

To investigate the roles of HK2 in normal B cell development and function, we utilized mice with B cell-specific inactivation of the HK2 gene. We confirmed HK2 deficiency in splenic B cells at the mRNA and protein levels, while HK1 and HK3 expression remained intact (Figure S1). We then performed intracellular flow cytometry analysis in various mouse tissues to estimate HK2 protein levels during B cell development and activation (flow gating illustrated in Figure S2). The specificity of the rabbit monoclonal anti-HK2 reagent used was validated using HK2-deficient activated mouse splenic B cells (Figure 3A). In the bone marrow, HK2 staining intensity is low in all B cell subsets with the exception of pro-B cells, which appear to express more HK2 than other B lineage subsets (Figure 3B). In the spleen, mature follicular B cells show the lowest HK2 staining intensity, with marginal zone and B1 populations exhibiting higher staining intensity (Figure 3C). In peritoneal wash, B1 cells also have higher HK2 staining intensity than B2 cells (Figure 3D). Interestingly, basal populations of $CD86^{+}$ B cells and GC cells in the spleen, mesenteric lymph nodes, and Peyer's patches showed substantially higher HK2 staining than resting B cells in these same tissues (Figure S3A). These results are relatively consistent with the levels of HK2 mRNA transcripts in B cell subsets as reported in the ImmGen database (Figure S3B).

While HK2-deficient mice exhibited normal frequencies of $CD19^{+}$ B cells in the spleen, peritoneal wash, mesenteric lymph nodes, and Peyer's patch, a small but significant reduction in B lineage cells within the bone marrow was noted (Figures 3E and S4A). Examination of B cell subsets in the bone marrow revealed that the reduced frequency of B lineage cells was due to significantly reduced pre-B and immature B cells (Figures 3F and 3G). While mature B cell subsets were present at normal frequencies in the spleen, a reduced frequency of transitional 2 B cells was observed in HK2-deficient mice (Figures 3H and 3I). Frequencies of spontaneous GCBs in mesenteric lymph node, Peyer's patch, and spleen were within normal ranges (Figure S4B) and B1a, B1b, and B2 cell subsets in peritoneal cavity were also not affected (Figure S4C). Basal serum levels of all antibody isotypes tested were within normal ranges, except IgM, which showed a small

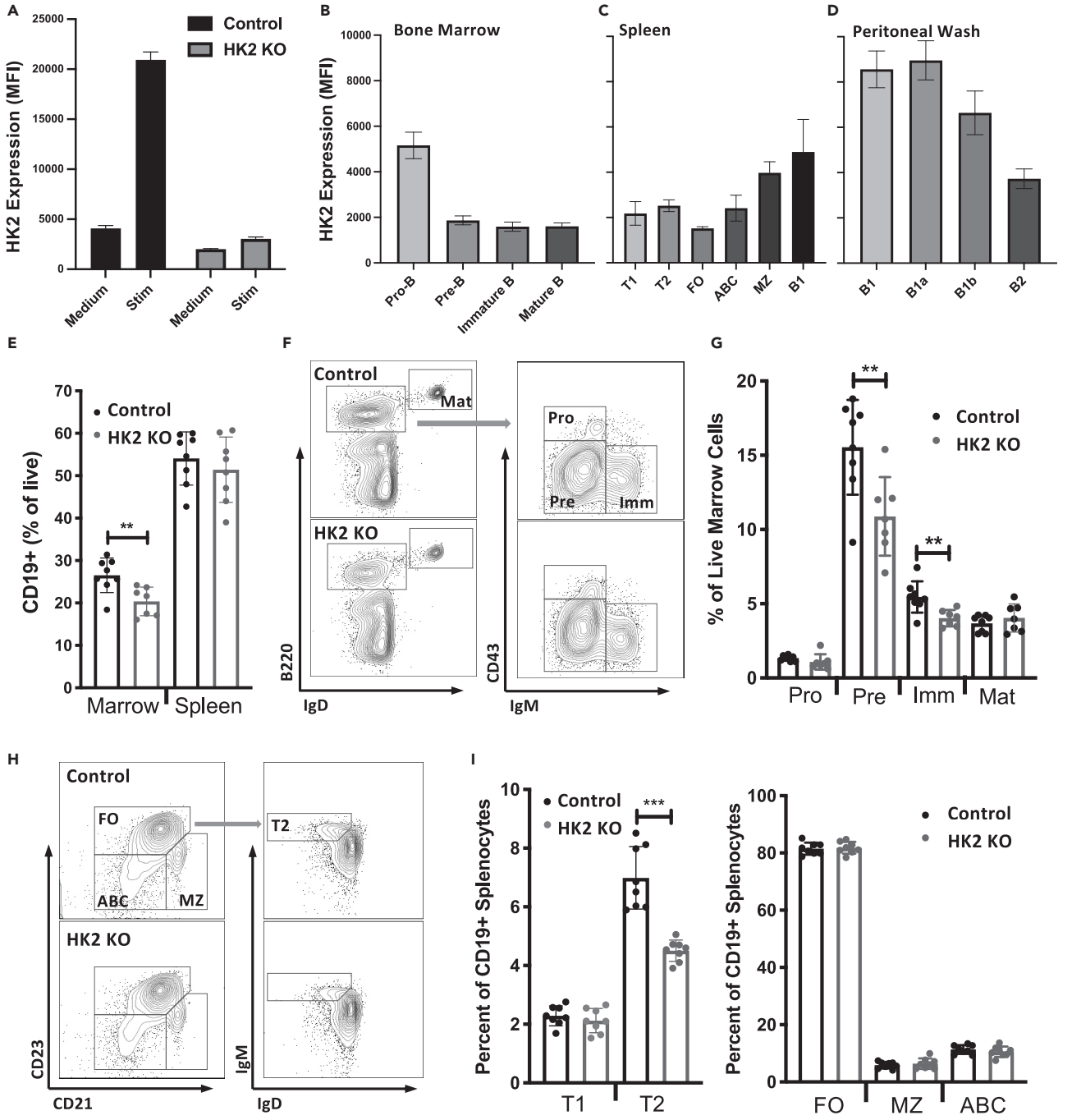

Figure 3. Roles of HK2 in B cell development

(A) Validation of HK2 intracellular staining specificity using activated HK2 KO B cells. Also see Figure S1.

(B–D) Single-cell suspensions from the indicated mouse tissues were surface stained to identify B cell sub-populations and intracellularly stained to assess HK2 expression. Background-subtracted HK2 MFIs were determined for each cell population. T1/T2, transitional 1/2; FO, follicular; ABC, age-associated B cell; MZ, marginal zone. Population gating is described in Figure S2. See Figure S3 for additional HK2 expression data. Graphs show mean and standard error of 5 mice per group and are representative of 2–3 experiments per tissue.

(E) Frequencies of $CD19^+$ B cells in the spleen and bone marrow.

(F) Representative flow cytometry plots illustrating gating in the bone marrow.

(G) Frequencies of B cell and precursor subsets in the bone marrow.

(H) Representative flow cytometry plots illustrating gating of $CD19^+$ B cell subsets in the spleen.

(I) Frequencies of immature and mature B cell subsets in the spleen. Results in (E–I) are pooled from two experiments, totaling 8 mice per genotype.

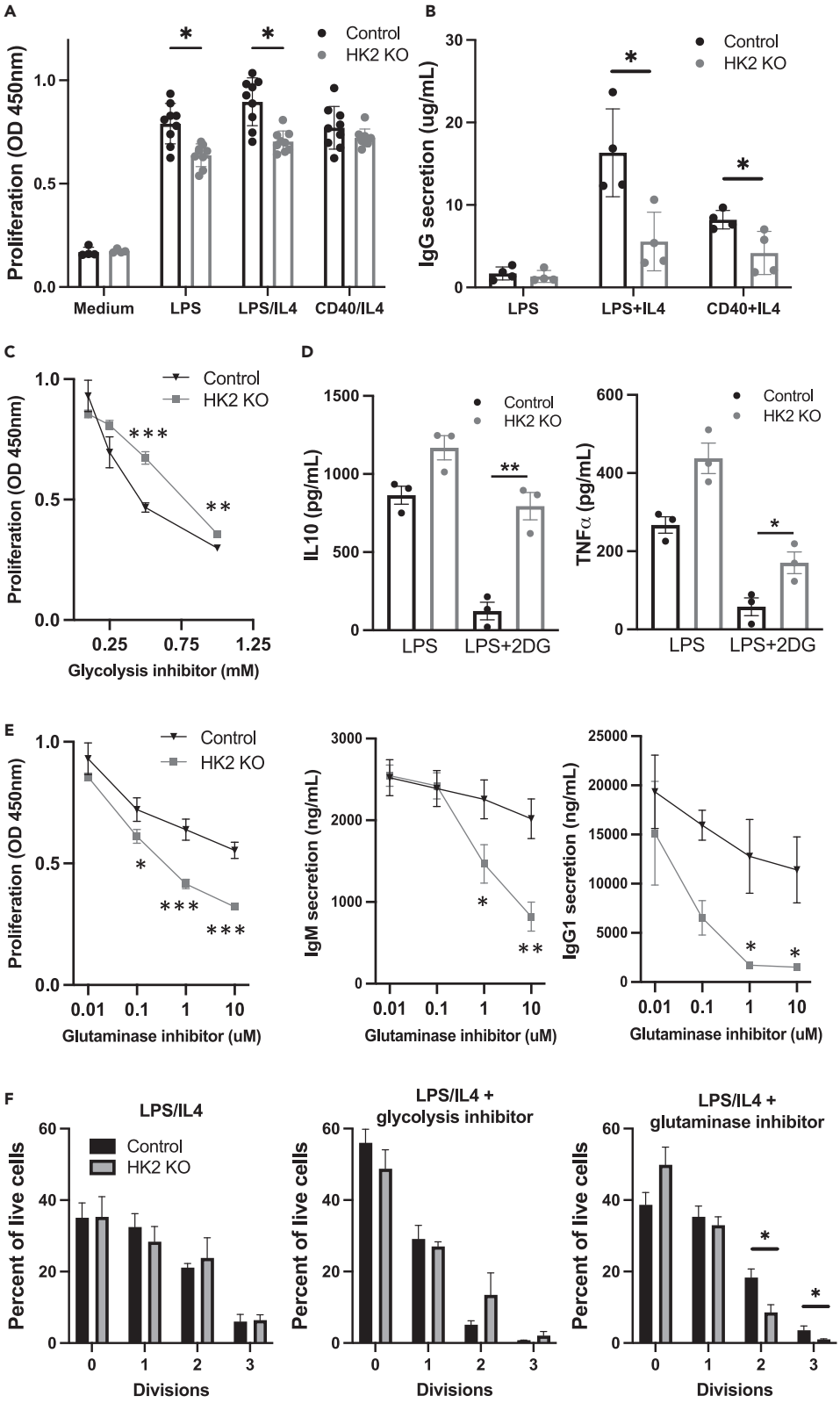
A
Proliferation (OD 450nm)
Control
HK2 KO
Medium
LPS
LPS/IL4
CD40/IL4
B
IgG secretion (ug/mL)
LPS
LPS+IL4
CD40+IL4
C
Proliferation (OD 450nm)
Glycolysis inhibitor (mM)
D
IL10 (pg/mL)
TNFα (pg/mL)
LPS
LPS+2DG
E
Proliferation (OD 450nm)
Glutaminase inhibitor (uM)
IgM secretion (ng/mL)
IgG1 secretion (ng/mL)
F
LPS/IL4
LPS/IL4 +
glycolysis inhibitor
LPS/IL4 +
glutaminase inhibitor
Percent of live cells
Divisions

Figure 4. HK2 deficiency impacts *in vitro* B cell functional responses

Splenic B cells were isolated from HK2-deficient or littermate control mice and cultured in the presence of the indicated activation stimuli.

(A) Proliferation was assessed at day 4 of culture by CCK-8 assay. Results are pooled from two experiments, totaling 8 mice per genotype.

(B) After 6 days of culture, supernatants were collected to measure secreted IgG1 antibodies by ELISA assay. The experiment shown (4 mice per genotype) is representative of 3 experiments with similar results.

(C) Cells were stimulated with LPS+IL-4 in the presence of the indicated concentrations of glycolysis inhibitor 2-deoxyglucose (2DG) and proliferation assessed. Results are representative of 3 independant experiments.

(D) Cells were stimulated with LPS alone or in the presence of 0.5 mM 2DG, and the indicated cytokines were assessed by Mesoscale assay. Results are from a single experiment (3 mice per genotype).

(E) Cells stimulated with LPS+IL-4 in the presence of the indicated concentrations glutaminase inhibitor CB-839 and proliferation or antibody secretion were assessed.

(F) Cells were labeled with cell division dye CFSE, stimulated with LPS+IL-4 with medium alone or in the presence of 0.5 mM 2DG or 1 μM CB-839, and analyzed by flow cytometry to gate cells based on CFSE dilution. Graphs show the percent of cells in the indicated cell division gates and represent data pooled from 4 mice per genotype. See Figure S4 for additional functional characterization of HK2-deficient mice.

decrease in HK2-deficient mice (Figure S4D). These results indicate that HK2 deficiency perturbs B cell development but does not block the generation of mature B cell subsets.

HK2 deficiency impacts B cell functional responses *in vitro*

B cells isolated from HK2-deleted B cells or littermate controls were activated overnight and their functional responses were assessed. We found that HK2-deficient B cells show slightly reduced response to lipopolysaccharide (LPS) or LPS+IL-4 as measured by cell counting kit assay, while the response to anti-CD40+IL-4 was not significantly affected (Figure 4A). HK2-deficient B cells showed markedly impaired IgG1 secretion with either LPS+IL-4 or CD40+IL-4 stimulation (Figure 4B), whereas IgM levels were reduced only with CD40+IL-4 stimulation (Figure S4E). To examine whether HK2 deficiency renders B cells more sensitive to glycolysis inhibition, we assessed the effect of glycolysis inhibitor 2DG. We unexpectedly found that HK2-deficient B cells were partially resistant to the inhibitory effects of 2DG, as measured by cell counting kit assay (Figure 4C) or production of cytokines (Figure 4D). This suggested that HK2-deficient B cells may undergo compensatory adaption of their metabolic network to be less dependent on glycolysis. Since glutamine is an additional important source of energy and biosynthetic precursors in activated lymphocytes, we examined the sensitivity of HK2-deficient B cells to the glutaminase inhibitor CB-839 (telaglenastat). Remarkably, HK2-deficient B cells are significantly more sensitive to glutaminase inhibition, showing greater reductions in proliferation, IgM secretion, and IgG1 secretion in the presence of CB-839 (Figure 4E). While HK2 knockout (KO) cells did not show significantly altered cell division profiles as assessed by CFSE dilution assay, their division was suppressed more strongly by glutaminase inhibitor (Figure 4F). Together, these results suggest that HK2 normally plays a significant role in B activation, but in the face of congenital HK2 deficiency, B cells metabolically adapt to reduce their dependence on glucose in part by increased utilization of glutamine as an alternative fuel source.

Impact of HK2 deficiency on B cell metabolite profiles

To determine how metabolic pathways are altered in HK2-deficient B cells, a panel of 84 metabolites in central carbon metabolism were measured by mass spectrometry, comparing splenic B cells from control or HK2-deficient mice cultured overnight in medium or stimulation cocktail (Figure 5A; Table S1). Both lactic acid and tricarboxylic acid (TCA) cycle intermediates were reduced in activated HK2-deficient cells (Figure 5A). As expected, G6P/glucose ratios were decreased in HK2-deficient cells, while glycolytic intermediate fructose-6-P was only modestly reduced relative to glucose (Figure 5B). PPP intermediate 6-phosphogluconate and glycogen synthesis intermediate glucose-1-P were both reduced relative to glucose (Figure 5B). Notably, HK2-deficient B cells exhibit substantial (1.5- to 4-fold) reductions in most nucleotides measured under resting conditions; however, this deficiency was largely overcome upon stimulation. After incubation of cells with ^{13}C-glucose, we assessed the extent of ^{13}C-labeling in a number of downstream metabolites. While no consistent differences in ^{13}C-labeling of glycolysis intermediates were observed, M+2 labeling of lactate was found to be decreased (Figure 5C). Subtle differences in labeling of TCA metabolites were observed in stimulated HK2 KO cells (Figure 5D); notably, citrate, isocitrate, alpha-ketoglutarate, and succinate all showed significant reductions in M+2 labeling, potentially reflecting a reduced proportion of glucose-derived carbons entering into the TCA. A sharp drop-off in ^{13}C-labeling between isocitrate and α-ketoglutarate was observed in both genotypes (from 40% to 50% down to 10%–20%), consistent with substantial influx of glutamine carbons into the TCA at this point. Overall, these findings suggest that HK2-deficient B cells have defects in glucose utilization affecting multiple anabolic and catabolic pathways.

Impact of HK2 deficiency on response to immunization

To further assess HK2 expression and function *in vivo*, mice were immunized with sheep red blood cells (SRBCs) to generate strong GC and plasmablast responses. GCBs and plasmablasts in the spleen displayed very high HK2 expression, peaking early in the response and maintained until day 8 (Figure 6A). Flow cytometry assessment at day 8 post immunization revealed significant alterations in activated cell populations in HK2-deficient mice, including reductions in CD86^{+} cells and GCBs (Figure 6B). Plasmablast frequencies were also reduced in the spleen and bone marrow of SRBC-immunized HK2-deficient mice (Figure 6C) and correspondingly, SRBC-binding IgM and IgG antibodies were significantly reduced at both day 5 and 10 post immunization (Figure 6D). Together, these results indicate that HK2 deficiency leads to significant impairments in B cell functional responses to SRBC immunization.

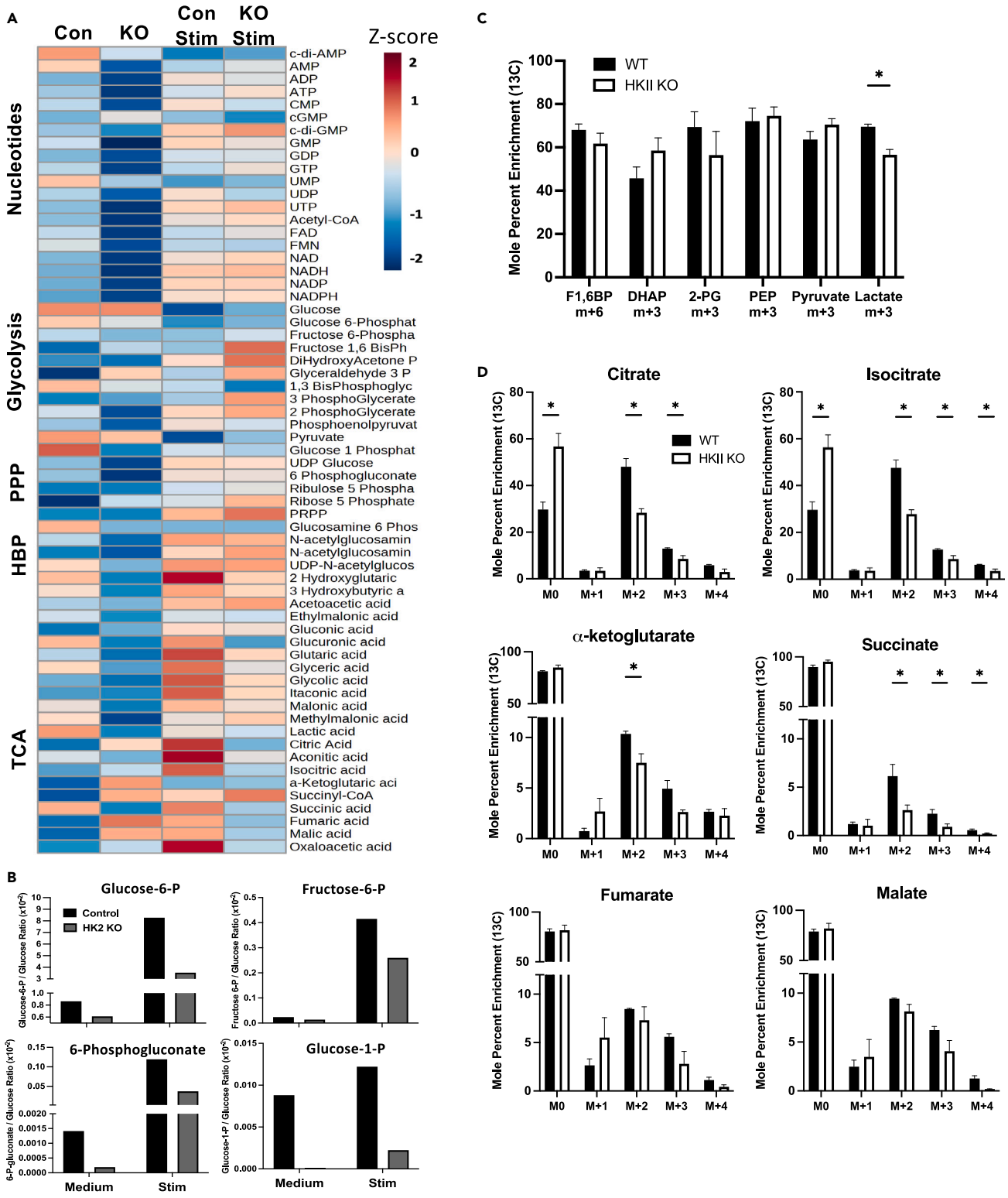

Figure 5. Impact of HK2 deficiency on metabolite profiles

Splenic B cells were cultured overnight in RPMI media only or with F(ab')2 anti-IgM, CD40L, and IL-4 (Stim), and then snap frozen. Metabolites were extracted, measured by mass spectrometry and normalized to total protein content in each sample.

(A) Heatmap illustrating relative differences in metabolite levels. Full metabolite profiling data is provided in Table S1.

Figure 5. *Continued*

(B) Calculated ratios of glucose-6-P, fructose-6-P, 6-phosphogluconate, or glucose-1-P to glucose under resting or activated conditions. Results in (A) and (B) are from a single experiment using 2 mice per genotype.

(C and D) Cells were stimulated overnight, washed in glucose-free medium, and incubated for 1 h (C) or 4 h (D) with ^{13}C-glucose to allow incorporation of ^{13}C into downstream metabolites. ^{13}C-labeled and unlabeled metabolites were measured by mass spectrometry and percent labeling of each metabolite is shown. F1,6BP, fructose-1,6-bisphosphate; DHAP, dihydroxyacetone phosphate; 2-PG, 2-phosphoglycerate; PEP, phosphoenolpyruvate. Results are pooled from 4 mice per genotype.

HK2 expression in malignant human B cells

B cell malignancies such as chronic lymphocytic leukemia (CLL) are known to be driven by chronic PI3K signaling[39] and exhibit metabolic reprogramming.[40,41] We thus assessed HK2 protein expression in a cohort of patients with CLL using flow cytometry (patient demographics and clinical information found in Table S2). Directly *ex vivo*, CLL cells show a trend of reduced HK2 expression compared to healthy control B cells (Figure 7A), potentially reflecting the predominantly quiescent phenotype of CLL cells in blood. We determined the association of CLL HK2 expression with various prognostic markers and found that it is significantly associated with ZAP70 expression (Figure 7B). While a trend of higher HK2 expression was observed in patients with unmutated IgVH, it was not associated with lymphocyte counts or B2M levels (Figure S5). Strikingly, higher HK2 expression was consistently seen within the proliferative fraction of CLL cells, characterized by low levels of surface CXCR4 and high expression of CD5 (Figure 7C).[42,43] Consistent with this, HK2 expression was inversely correlated with surface CXCR4 level (Figure 7D). Finally, we cultured CLL cells overnight with an activation cocktail, with or without PI3K inhibitor, and found significant reduction in HK2 expression upon PI3K inhibitor treatment (Figure 7E). These results suggest that HK2 expression may be upregulated by activation signals within lymphoid tissues and subsequently diminish in long-lived quiescent CLL cells in the blood.

DISCUSSION

It is well established that B cell activation increases glycolysis and this has largely been attributed to the elevation of the glucose transporter Glut1 and increased glucose uptake. Our study provides multiple lines of evidence indicating that the increase in glycolysis upon B cell activation is also associated with selectively increased expression and activity of HK2. As the first enzyme to act upon glucose entering the cell, HKs play a critical role, as conversion to G6P prevents export and irreversibly directs glucose into multiple downstream anabolic and catabolic pathways. Although B cells constitutively express HK1, our results indicate that activated B cells predominantly express HK2 and are functionally dependent on this enzyme to maximally activate glucose-dependent metabolism. Our study indicates that signaling through the PI3K pathway, and PI3Kδ specifically, is involved in reprogramming of HK isoforms, in addition to the previously reported role of PI3K in regulating Glut1 expression. The functional importance of HK2 is underlined by our findings that HK2-deficient B cells have impaired responses to stimulation *in vitro* and *in vivo*, despite showing evidence of metabolic reprogramming to reduce their dependence on glucose.

Substantial literature has implicated the PI3K signaling pathway in metabolic reprogramming in multiple cell types. In many cases, the evidence is based on pan-PI3K inhibitors or gain-of-function approaches of limited specificity. Our data specifically implicate PI3Kδ in activation-induced increase in glycolysis and elevation of HK2 expression. The mechanisms linking PI3K to glycolysis have been proposed to include Akt-dependent upregulation of Glut1, primarily based on experiments overexpressing membrane-targeted Akt.[31,44–46] The PI3K pathway is also closely intertwined with mTOR activation,[47] which is a critical regulator of cellular metabolism.[48,49] Our results suggest that mTORC1 does play a role in HK2 upregulation in B cells, whereas Akt kinase activity is surprisingly not required. We have previously confimed that the inhibitors used strongly block Akt phosphorylation and activity in B cells,[8] and thus conclude that Akt kinase activity does not play an essential non-redundant role under the activation conditions used here. PI3K can also play a role in the upregulation of c-myc, which is a key driver of glycolytic gene expression, including HK2[50–52]; thus, c-myc may also contribute to the PI3K-dependent upregulation we observe here.

While all HK isoforms catalyze the same reaction, they differ in expression pattern, structure, enzyme kinetics, and subcellular localization. Unlike other isoforms, HK2 has two functional catalytic domains but a relatively low affinity for glucose,[53] and is thus expected to be most important when cells are highly active in taking up glucose. While HK1 is mainly localized to mitochondria and HK3 is mainly cytoplasmic, HK2 is found in both mitochondria and cytoplasm. Consistent with studies in Chinese hamster ovary cells,[54] we found that HK2 shows lower association with mitochondria in low glucose conditions but this is elevated upon activation of the PI3K pathway, indicating an additional layer of regulation beyond protein expression levels. This could be due in part to phosphorylation of HK2 by Akt, which was reported to enhance HK2 mitochondrial association[19]; however, other kinases such as PIM2 may also serve this function,[55] and constitutively active Akt does not significantly increase mitochondrial HK activity.[45] Several studies have found that dissociating HK2 from mitochondria can trigger mitochondrial dysfunction, disrupted calcium homeostasis, and cell death in some contexts,[56] indicating the functional importance of HK2 mitochondrial association. A recent study found that HK1 can also undergo regulated translocation between mitochondria and cytoplasm in macrophages, and found that mitochondrial localization of HK1 was functionally important for macrophage activation.[36] Together, the current evidence indicates that PI3K and other signaling pathways can reprogram both HK isoform expression and subcellular localization, likely impacting the utilization of glucose in different downstream metabolic pathways.

Our assessment of HK2 protein expression in B cell subsets indicates it could potentially have roles in B cell development including at the pro-B and transitional B cell stages. It should be noted that differential binding of other fluorochrome-labeled phenotyping antibodies to each cell subset could potentially impact the fluorescence signals used to estimate HK2 expression; however, we also noted elevated levels of HK2 mRNA in pro-B and transitional B cell populations in Figure S3. While HK2 is not essential for B cell development, HK2 KO mice exhibit

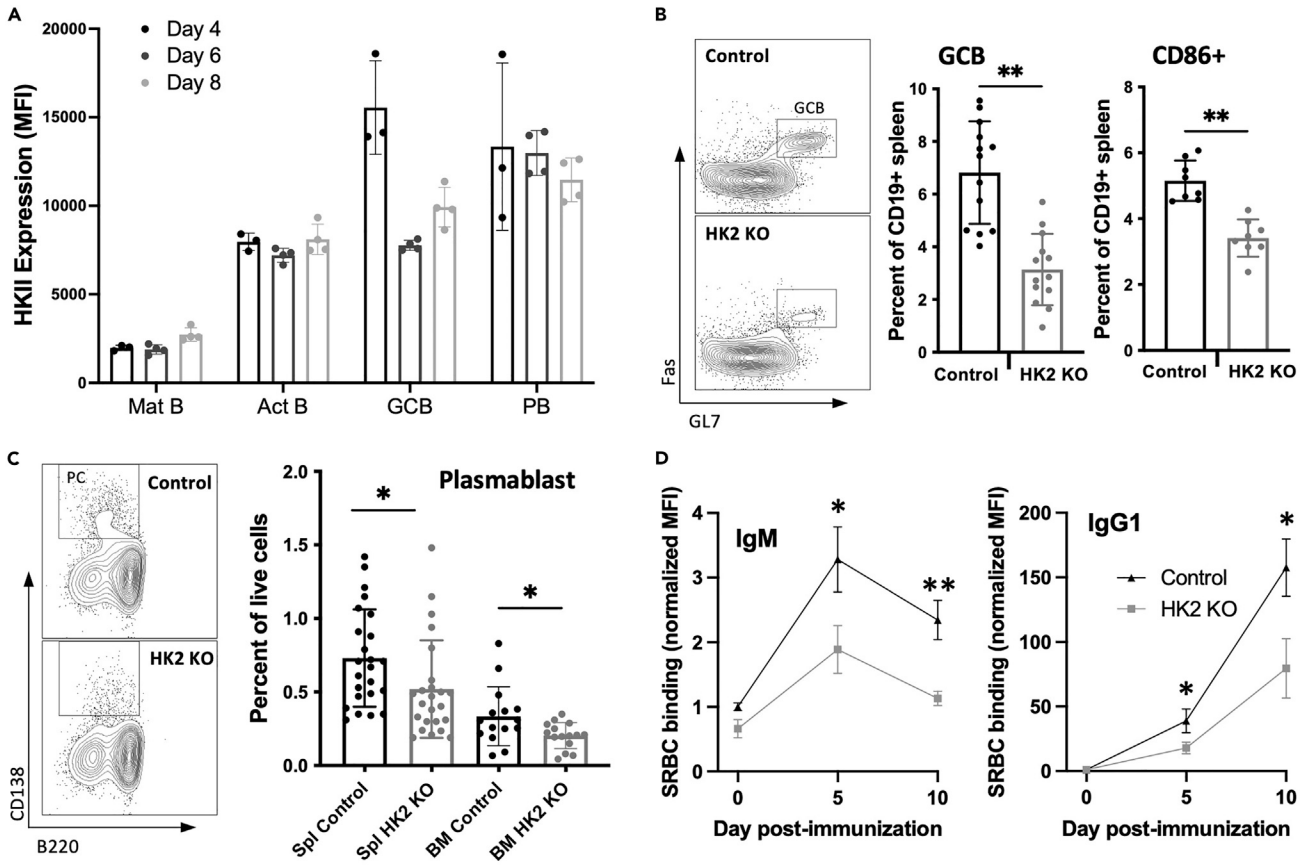

Figure 6. Effect of B cell-specific HK2 deficiency on responses to immunization

HK2-deficient or littermate control mice were immunized with sheep red blood cells (SRBCs) and assessed by flow cytometry.

(A) HK2 expression in activated B cell populations generated at the indicated time points after SRBC immunization.

(B) Representative flow cytometry plots illustrating gating of germinal center B cell populations in spleen and graphs showing frequencies of germinal center B cells and CD86^{+} B cells pooled from 2 to 3 experiments.

(C) Representative flow cytometry plots illustrating gating of plasma cell populations in the spleen and bone marrow and graph showing cell frequencies pooled from 5 experiments.

(D) Generation of SRBC-binding IgM and IgG antibodies. SRBC were incubated with serum from the indicated days post immunization, and bound antibodies were detected by immunofluorescence staining and flow cytometry. Results are representative of 4 similar experiments. Significance was determined by t test (*$p < 0.05$; **$p < 0.005$).

mild impairments in key developmental transitions known to be dependent on B cell receptor (BCR) signaling and the PI3K pathway. We see significant reductions in bone marrow pre-B cells and spleen transitional 2 cells, known to depend on pre-BCR or BCR signaling, respectively. Although B1 and marginal zone B cells showed higher levels of HK2 than follicular B cells, all of these mature B cell populations were present at normal frequencies in HK2-deficient mice. This indicates that the mild impairment in lymphocyte development does not prevent mature B cell compartments from eventually reaching their normal homeostatic levels by adulthood. It is possible that metabolic plasticity allows proliferative pre-B cell subsets to adapt their metabolic pathways sufficiently to compensate for the absence of HK2. We did not observe substantial compensatory increases in HK1 or HK3 expression, although a trend of marginally increased HK3 was noted in splenic B cells. Together, our results are more consistent with metabolic adaptations that reduce B cell dependence on glucose, and potentially increase their dependence on other sources of energy and metabolic building blocks such as amino acids or other sugars.

We find that the deletion of HK2 in human lymphoma cells or primary mouse B cells substantially reduced ECAR upon glucose addition, despite continued expression of HK1 and HK3. This indicates that HK2 plays an essential non-redundant role in maximizing glycolytic capacity that is not easily compensated. HK2-deficient mouse B cells show mildly impaired responses to LPS measured using the CCK-8 proliferation assay, but no significant reduction in cell division measured by CFSE dilution. As the CCK-8 assay measures a formazan product generated via the activity of cellular dehydrogenases, the observed reduction could be related to either altered metabolic state of the cells or reduced cell survival of HK2 KO cells in these cultures. As the generation of IgG1 responses *in vitro* involves a number of factors, including division-linked antibody isotype switch and PC differentiation, the observed reduction in IgG1 production could reflect impairments in one or more of these processes. Given that cell division appears unaffected, and IgM levels were also observed to be decreased in some conditions *in vitro* and

in vivo, it seems more likely to relate to decreased PC differentiation or survival. Strikingly, HK2 KO B cells were found to be more sensitive to glutaminase inhibition based on multiple functional assays (CCK-8, CFSE, or IgG1 secretion), indicating that these cells have adapted to become less dependent on glycolysis and instead rely more on glutaminolysis. This adaptation illustrates an unexpected level of metabolic plasticity in B cell responses, which may somewhat obscure the normal roles of HK2 when cells are cultured in media with abundant glucose and glutamine.

HK2 deficiency significantly impacted metabolite profiles of splenic B cells, again demonstrating that this enzyme has metabolic functions which cannot be fully compensated by HK1/3. As metabolite levels are influenced both by rates of production and consumption, the interpretation of these data is complex. For example, glucose levels are found to substantially decrease upon B cell activation, despite known increases in glucose uptake, presumably reflecting more rapid consumption by phosphorylation into G6P and utilization in downstream pathways. Consistent with reduction in ECAR, both lactic acid levels and ^{13}C-glucose labeling of lactate were reduced in activated HK2 KO cells compared to controls. Entry of glucose into the TCA cycle also appears to be reduced based on ^{13}C-glucose labeling of citrate and isocitrate. While HK2 KO cells were found to have significantly decreased levels of nucleotides, intermediates in utilization of glucose for nucleotide synthesis, such as ribose-5-P and PRPP, were not decreased; this might reflect decreased consumption of these metabolites due to impaired activity of the pentose phosphate pathway (PPP). Consistent with this interpretation, HK2-deficient cells show reduced 6-phosphogluconate/glucose ratios suggesting an impairment in the first step of glucose entry into the PPP. Glucose conversion into glucose-1-P, the first step in glycogen synthesis, also appeared to be severely impacted by HK2 deficiency based on low glucose-1-P/glucose ratios. While little is known about the role of glycogen storage in lymphocytes, they do express glycogen synthase, contain measurable stores of glycogen, and have functional insulin receptors.[57,58] Together, our results indicate that HK2 deficiency substantially impairs glucose utilization in anabolic and catabolic pathways, and may impact glucose storage.

Upon immunization with SRBCs, we found that B cell-specific HK2 deficiency caused a significant reduction in both GC B cells and PCs. This is consistent with the observed elevation in HK2 protein levels in GCB and PCs and suggests these cells may be particularly dependent on HK2 activity. Several studies have indicated that the GC is a hypoxic environment, and consequently GCB increase their activation of glycolysis pathways[5,14]; however, other studies have highlighted the importance of oxidative phosphorylation in GCBs.[14,59] Interestingly, a recent study examining lactate dehydrogenase-deficient B cell responses concluded that aerobic glycolysis is most important in early (day 4) pre-GC GL7+ cells.[60] As we noted that HK2 expression within GC phenotype cells peaked at day 4 post immunization, it is likely that HK2 helps drive glycolysis at this stage. PCs are known to exhibit high glucose utilization, with a large fraction being utilized for protein glycosylation.[20] Thus, it is possible that the defective antibody responses we observe relate to impaired PC generation, survival, and/or reduced ability to secrete antibody.

The *in vivo* functional impact of reducing glucose transport in B cells has recently been studied using B cell-specific Glut1 KO mice. These mice show phenotypes overlapping with our findings, including sub-optimal GCB and PC responses.[61,62] Bierling et al. found that Glut1 deficiency impairs multiple metabolic pathways including glycolysis, TCA, PPP, and hexosamine biosynthetic pathway,[62] underlining the importance of glucose uptake in supporting both anabolic and catabolic metabolism. Interestingly, Brookens et al. found that the requirement for glucose uptake to sustain PC responses *in vitro* could be compensated by the addition of other hexoses (galactose and mannose)[61]; thus, glucose may not be absolutely required if sufficient supply of other sugars is available to sustain high-level production of glycosylated antibodies.

While human B lymphoma lines such as BJAB constitutively express very high levels of HK2, primary CLL cells in the blood did not exhibit elevated HK2 levels compared to normal human B cells. This is consistent with studies showing that the bulk of blood CLL cells are quiescent and rely mainly on mitochondrial lipid oxidation.[63] However, we found evidence that the recently proliferated fraction of CLL has markedly elevated levels of HK2, suggesting that actively dividing CLL cells may upregulate HK2 and enhance glucose utilization within lymph node proliferation centers. This upregulation may occur in response to activation signals present in the lymphoid tissue microenvironent that trigger the PI3K pathway.[64]

Together, our results suggest that acute inhibition of HK2 activity could be applied to selectively inhibit GC and PC responses as well as the proliferation of malignant B cells. Indeed, 2DG treatment *in vivo* has been found to disrupt chronic GCs and reduce autoantibody generation *in vivo*,[8,65] which may be in part attributable to direct effects on GCBs and PCs. However, given the metabolic plasticity observed in this study, combined inhibition of HK2 and other compensatory pathways may be more effective.

Limitations of the study

Several components of our study rely on genetic tools to constitutively inactivate the HK2 gene. During culture of cell lines or development of B cells *in vivo*, metabolic adaptations may occur to allow cell survival and proliferation. As a result, the role of HK2 in B cell activation and metabolism may be underestimated. Limitations of specific experimental approaches for assessing HK2 function are discussed earlier.

RESOURCE AVAILABILITY

Lead contact

Further information and requests for resources and reagents should be directed to and will be fulfilled by the lead contact, Aaron Marshall (aaron.marshall@umanitoba.ca).

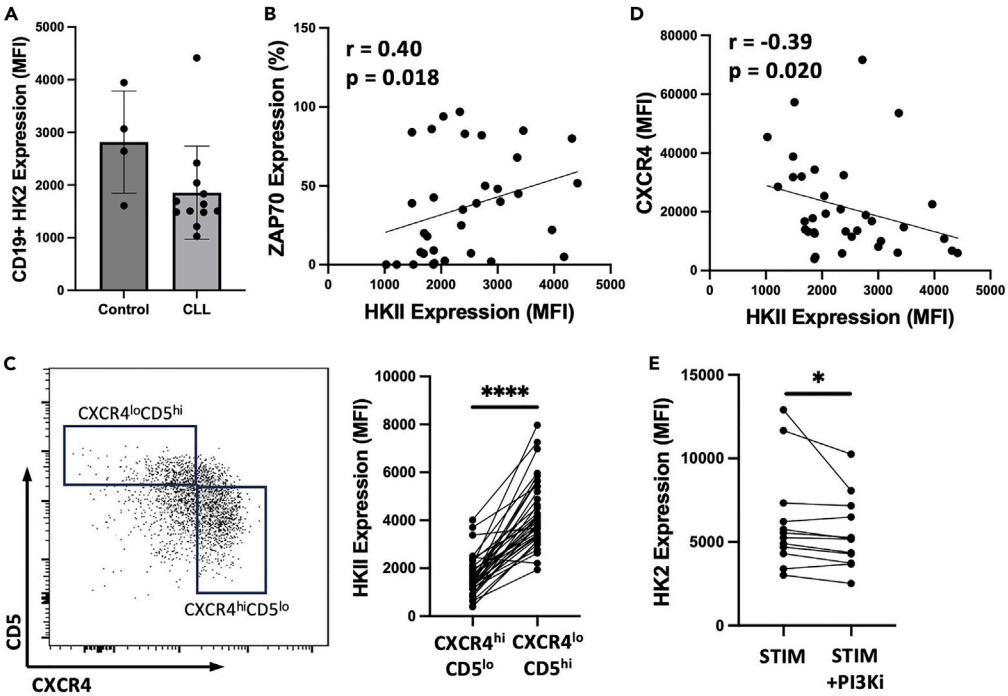

Figure 7. Expression of HK2 in B cell leukemia

Peripheral blood mononuclear cell samples from patients with chronic lymphocytic leukemia or healthy controls were assessed for HK2 expression by flow cytometry.

(A) HK2 MFI within gated $CD19^+$ cells. Each dot represents an individual patient or healthy control.

(B) Spearman's correlation of HK2 MFI with percent ZAP70 expression among CLL cells (determined by clinical lab testing).

(C) Proliferative versus quiescent CLL cell populations were gated based on CXCR4 and CD5 expression (left). HK2 expression in each individual patient's proliferative and quiescent cell fractions are connected by lines (right). Significance was determined by Wilcoxon test.

(D) Pearson's correlation of HK2 MFI with CXCR4 expression among CLL cells. See Table S2 for CLL patient demographics and clinical parameters and Figure S5 for the association of HK2 expression with other CLL clinical parameters.

(E) CLL cells were cultured overnight with CD40L+IL-4+anti-IgM (Stim) alone or with pan-PI3K inhibitor (1 μM pictilisib) prior to assessment of HK2 expression. Significance was determined by Wilcoxon test.

Materials availability

HK2-deficient BJAB cells and HK2-deficient mice are available upon request to the lead contact.

Data and code availability

- Data produced in this paper are available upon request to the lead contact.
- This paper does not report original code.
- Any additional information required to reanalyze the data reported in this paper is available from the lead contact upon request.

ACKNOWLEDGMENTS

This work was funded by the Canadian Institutes of Health Research (project grant #162268). Critical infrastructure was funded by the Canadian Foundation for Innovation. B.T.P. was funded by a studentship from the Natural Sciences and Engineering Council of Canada. E.M.M. was funded by a fellowship from Research Manitoba and CancerCare Manitoba. F.O.-A. was supported by a studentship from Research Manitoba.

AUTHOR CONTRIBUTIONS

B.T.P.: methodology, investigation, validation, visualization, formal analysis, and writing – original draft; S.H.: methodology, investigation, validation, visualization, and formal analysis; E.M.M.: conceptualization, methodology, investigation, validation, and visualization; F.O.-A.: methodology and validation; D.F.: methodology and validation; G.M.H.: resources and supervision; A.S.: resources and supervision; V.B.: resources and data curation; N.H.: resources; H.Z.: methodology, investigation, and validation; A.J.M.: funding acquisition, conceptualization, visualization, formal analysis, and writing – review and editing.

DECLARATION OF INTERESTS

The authors declare no competing interests.

STAR★METHODS

Detailed methods are provided in the online version of this paper and include the following:

- KEY RESOURCES TABLE
- EXPERIMENTAL MODEL AND STUDY PARTICIPANT DETAILS
  - Mice
  - Human samples and clinical biomarkers
  - Cell culture
- METHOD DETAILS
  - Crispr deletion of HK2
  - RT-qPCR
  - Western blots
  - Confocal microscopy analysis of mitochondrial localization
  - Metabolic flux assays
  - Flow cytometry
  - Mouse immunization and antibody measurements
  - *In vitro* B cell proliferation and antibody secretion assays
  - Metabolite profiling
  - ^{13}C-glucose labeling and mass spectrometry
- QUANTIFICATION AND STATISTICAL ANALYSES

SUPPLEMENTAL INFORMATION

Supplemental information can be found online at https://doi.org/10.1016/j.isci.2024.110939.

Received: March 7, 2024
Revised: July 12, 2024
Accepted: September 10, 2024
Published: September 13, 2024

REFERENCES

1. Warburg, O. (1956). On the Origin of Cancer Cells. Am. Assoc. Adv. Sci. *123*, 309–314.
2. Boothby, M.R., Brookens, S.K., Raybuck, A.L., and Cho, S.H. (2022). Supplying the trip to antibody production—nutrients, signaling, and the programming of cellular metabolism in the mature B lineage. Cell. Mol. Immunol. *19*, 352–369. https://doi.org/10.1038/s41423-021-00782-w.
3. Jellusova, J. (2020). Metabolic control of B cell immune responses. Curr. Opin. Immunol. *63*, 21–28. https://doi.org/10.1016/j.coi.2019.11.002.
4. Khalsa, J.K., Chawla, A.S., Prabhu, S.B., Vats, M., Dhar, A., Dev, G., Das, N., Mukherjee, S., Tanwar, S., Banerjee, H., et al. (2019). Functionally significant metabolic differences between B and T lymphocyte lineages. Immunology *158*, 104–120. https://doi.org/10.1111/imm.13098.
5. Jellusova, J., Cato, M.H., Apgar, J.R., Ramezani-Rad, P., Leung, C.R., Chen, C., Richardson, A.D., Conner, E.M., Benschop, R.J., Woodgett, J.R., and Rickert, R.C. (2017). Gsk3 is a metabolic checkpoint regulator in B cells. Nat. Immunol. *18*, 303–312. https://doi.org/10.1038/ni.3664.
6. Doughty, C.A., Bleiman, B.F., Wagner, D.J., Dufort, F.J., Mataraza, J.M., Roberts, M.F., and Chiles, T.C. (2006). Antigen receptor–mediated changes in glucose metabolism in B lymphocytes: role of phosphatidylinositol 3-kinase signaling in the glycolytic control of growth. Blood *107*, 4458–4465. https://doi.org/10.1182/blood-2005-12-4788.
7. Jellusova, J., and Rickert, R.C. (2016). The PI3K pathway in B cell metabolism. Crit. Rev. Biochem. Mol. Biol. *51*, 359–378. https://doi.org/10.1080/10409238.2016.1215288.
8. Jayachandran, N., Mejia, E.M., Sheikholeslami, K., Sher, A.A., Hou, S., Hatch, G.M., and Marshall, A.J. (2018). TAPP Adaptors Control B Cell Metabolism by Modulating the Phosphatidylinositol 3-Kinase Signaling Pathway: A Novel Regulatory Circuit Preventing Autoimmunity. J. Immunol. *201*, 406–416. https://doi.org/10.4049/jimmunol.1701440.
9. Akkaya, M., Traba, J., Roesler, A.S., Miozzo, P., Akkaya, B., Theall, B.P., Sohn, H., Pena, M., Smelkinson, M., Kabat, J., et al. (2018). Second signals rescue B cells from activation-induced mitochondrial dysfunction and death. Nat. Immunol. *19*, 871–884. https://doi.org/10.1038/s41590-018-0156-5.
10. Waters, L.R., Ahsan, F.M., Wolf, D.M., Shirihai, O., and Teitell, M.A. (2018). Initial B Cell Activation Induces Metabolic Reprogramming and Mitochondrial Remodeling. iScience *5*, 99–109. https://doi.org/10.1016/j.isci.2018.07.005.
11. Caro-Maldonado, A., Wang, R., Nichols, A.G., Kuraoka, M., Milasta, S., Sun, L.D., Gavin, A.L., Abel, E.D., Kelsoe, G., Green, D.R., and Rathmell, J.C. (2014). Metabolic reprogramming is required for antibody production that is suppressed in anergic but exaggerated in chronically BAFF-exposed B cells. J. Immunol. *192*, 3626–3636. https://doi.org/10.4049/jimmunol.1302062.
12. Patke, A., Mecklenbräuker, I., Erdjument-Bromage, H., Tempst, P., and Tarakhovsky, A. (2006). BAFF controls B cell metabolic fitness through a PKC beta- and Akt-dependent mechanism. J. Exp. Med. *203*, 2551–2562.
13. Abbott, R.K., Thayer, M., Labuda, J., Silva, M., Philbrook, P., Cain, D.W., Kojima, H., Hatfield, S., Sethumadhavan, S., Ohta, A., et al. (2016). Germinal Center Hypoxia Potentiates Immunoglobulin Class Switch Recombination. J. Immunol. *197*, 4014–4020. https://doi.org/10.4049/jimmunol.1601401.
14. Cho, S.H., Raybuck, A.L., Stengel, K., Wei, M., Beck, T.C., Volanakis, E., Thomas, J.W., Hiebert, S., Haase, V.H., and Boothby, M.R. (2016). Germinal centre hypoxia and regulation of antibody qualities by a hypoxia response system. Nature *537*, 234–238. https://doi.org/10.1038/nature19334.
15. Raybuck, A.L., Cho, S.H., Li, J., Rogers, M.C., Lee, K., Williams, C.L., Shlomchik, M., Thomas, J.W., Chen, J., Williams, J.V., and Boothby, M.R. (2018). B Cell-Intrinsic mTORC1 Promotes Germinal Center-Defining Transcription Factor Gene Expression, Somatic Hypermutation, and Memory B Cell Generation in Humoral Immunity. J. Immunol. *200*, 2627–2639. https://doi.org/10.4049/jimmunol.1701321.
16. Dominguez-Sola, D., Victora, G.D., Ying, C.Y., Phan, R.T., Saito, M., Nussenzweig, M.C., and Dalla-Favera, R. (2012). The proto-oncogene MYC is required for selection in the germinal center and cyclic reentry. Nat. Immunol. *13*, 1083–1091. https://doi.org/10.1038/ni.2428.
17. Ersching, J., Efeyan, A., Mesin, L., Jacobsen, J.T., Pasqual, G., Grabiner, B.C., Dominguez-Sola, D., Sabatini, D.M., and Victora, G.D. (2017). Germinal Center Selection and Affinity Maturation Require Dynamic Regulation of mTORC1 Kinase. Immunity *46*, 1045–1058.e6. https://doi.org/10.1016/j.immuni.2017.06.005.
18. Corcoran, L.M., and Nutt, S.L. (2016). Long-Lived Plasma Cells Have a Sweet Tooth. Immunity *45*, 3–5. https://doi.org/10.1016/j.immuni.2016.07.003.
19. Roberts, D.J., and Miyamoto, S. (2015). Hexokinase II integrates energy metabolism and cellular protection: Akting on mitochondria and TORCing to autophagy. Cell Death Differ. *22*, 248–257. https://doi.org/10.1038/cdd.2014.173.
20. Lam, W.Y., Becker, A.M., Kennerly, K.M., Wong, R., Curtis, J.D., Llufrio, E.M., McCommis, K.S., Fahrmann, J., Pizzato, H.A.,

Nunley, R.M., et al. (2016). Mitochondrial pyruvate import promotes long-term survival of antibody-secreting plasma cells. Immunity *45*, 60–73. https://doi.org/10.1016/j.immuni.2016.06.011.
21. Okkenhaug, K. (2013). Signaling by the phosphoinositide 3-kinase family in immune cells. Annu. Rev. Immunol. *31*, 675–704. https://doi.org/10.1146/annurev-immunol-032712-095946.
22. Fruman, D.A., Chiu, H., Hopkins, B.D., Bagrodia, S., Cantley, L.C., and Abraham, R.T. (2017). The PI3K Pathway in Human Disease. Cell *170*, 605–635. https://doi.org/10.1016/j.cell.2017.07.029.
23. Fruman, D.A. (2004). Phosphoinositide 3-kinase and its targets in B-cell and T-cell signaling. Curr. Opin. Immunol. *16*, 314–320.
24. Balla, T. (2013). Phosphoinositides: tiny lipids with giant impact on cell regulation. Physiol. Rev. *93*, 1019–1137. https://doi.org/10.1152/physrev.00028.2012.
25. Lemmon, M.A. (2007). Pleckstrin homology (PH) domains and phosphoinositides. Biochem. Soc. Symp. *74*, 81–93.
26. Limon, J.J., and Fruman, D.A. (2012). Akt and mTOR in B Cell Activation and Differentiation. Front. Immunol. *3*, 228.
27. Memmott, R.M., and Dennis, P.A. (2009). Akt-dependent and independent mechanisms of mTOR regulation in cancer. Cell. Signal. *21*, 656–664. https://doi.org/10.1016/j.cellsig.2009.01.004.
28. Zhu, Z., Shukla, A., Ramezani-Rad, P., Apgar, J.R., and Rickert, R.C. (2019). The AKT isoforms 1 and 2 drive B cell fate decisions during the germinal center response. Life Sci. Alliance *2*, e201900506. https://doi.org/10.26508/lsa.201900506.
29. Dufort, F.J., Bleiman, B.F., Gumina, M.R., Blair, D., Wagner, D.J., Roberts, M.F., Abu-Amer, Y., and Chiles, T.C. (2007). Cutting Edge: IL-4-Mediated Protection of Primary B Lymphocytes from Apoptosis via Stat6-Dependent Regulation of Glycolytic Metabolism. J. Immunol. *179*, 4953–4957. https://doi.org/10.4049/jimmunol.179.8.4953.
30. Maratou, E., Dimitriadis, G., Kollias, A., Boutati, E., Lambadiari, V., Mitrou, P., and Raptis, S.A. (2007). Glucose transporter expression on the plasma membrane of resting and activated white blood cells. Eur. J. Clin. Invest. *37*, 282–290. https://doi.org/10.1111/j.1365-2362.2007.01786.x.
31. Wieman, H.L., Wofford, J.A., and Rathmell, J.C. (2007). Cytokine stimulation promotes glucose uptake via phosphatidylinositol-3 kinase/Akt regulation of Glut1 activity and trafficking. Mol. Biol. Cell *18*, 1437–1446. https://doi.org/10.1091/mbc.e06-07-0593.
32. Nawaz, M.H., Ferreira, J.C., Nedyalkova, L., Zhu, H., Carrasco-López, C., Kirmizialtin, S., and Rabeh, W.M. (2018). The catalytic inactivation of the N-half of human hexokinase 2 and structural and biochemical characterization of its mitochondrial conformation. Biosci. Rep. *38*, BSR20171666. https://doi.org/10.1042/BSR20171666.
33. Robey, R.B., and Hay, N. (2006). Mitochondrial hexokinases, novel mediators of the antiapoptotic effects of growth factors and Akt. Oncogene *25*, 4683–4696. https://doi.org/10.1038/sj.onc.1209595.
34. Rodríguez-Saavedra, C., Morgado-Martínez, L.E., Burgos-Palacios, A., King-Díaz, B., López-Coria, M., and Sánchez-Nieto, S. (2021). Moonlighting Proteins: The Case of the Hexokinases. Front. Mol. Biosci. *8*, 701975. https://doi.org/10.3389/fmolb.2021.701975.
35. Varanasi, S.K., Jaggi, U., Hay, N., and Rouse, B.T. (2018). Hexokinase II may be dispensable for CD4 T cell responses against a virus infection. PLoS One *13*, e0191533. https://doi.org/10.1371/journal.pone.0191533.
36. De Jesus, A., Keyhani-Nejad, F., Pusec, C.M., Goodman, L., Geier, J.A., Stoolman, J.S., Stanczyk, P.J., Nguyen, T., Xu, K., Suresh, K.V., et al. (2022). Hexokinase 1 cellular localization regulates the metabolic fate of glucose. Mol. Cell *82*, 1261–1277.e9. https://doi.org/10.1016/j.molcel.2022.02.028.
37. Roberts, D.J., Tan-Sah, V.P., Smith, J.M., and Miyamoto, S. (2013). Akt Phosphorylates HK-II at Thr-473 and Increases Mitochondrial HK-II Association to Protect Cardiomyocytes. J. Biol. Chem. *288*, 23798–23806. https://doi.org/10.1074/jbc.M113.482026.
38. Wray-Dutra, M.N., Al Qureshah, F., Metzler, G., Oukka, M., James, R.G., and Rawlings, D.J. (2018). Activated PIK3CD drives innate B cell expansion yet limits B cell-intrinsic immune responses. J. Exp. Med. *215*, 2485–2496. https://doi.org/10.1084/jem.20180617.
39. Hoellenriegel, J., Meadows, S.A., Sivina, M., Wierda, W.G., Kantarjian, H., Keating, M.J., Giese, N., O'Brien, S., Yu, A., Miller, L.L., et al. (2011). The phosphoinositide 3'-kinase delta inhibitor, CAL-101, inhibits B-cell receptor signaling and chemokine networks in chronic lymphocytic leukemia. Blood *118*, 3603–3612. https://doi.org/10.1182/blood-2011-05-352492.
40. Vangapandu, H.V., Havranek, O., Ayres, M.L., Kaipparettu, B.A., Balakrishnan, K., Wierda, W.G., Keating, M.J., Davis, R.E., Stellrecht, C.M., and Gandhi, V. (2017). B-cell Receptor Signaling Regulates Metabolism in Chronic Lymphocytic Leukemia. Mol. Cancer Res. *15*, 1692–1703. https://doi.org/10.1158/1541-7786.MCR-17-0026.
41. Roy Chowdhury, S., Bouchard, E.D.J., Saleh, R., Nugent, Z., Peltier, C., Mejia, E., Hou, S., McFall, C., Squires, M., Hewitt, D., et al. (2020). Mitochondrial Respiration Correlates with Prognostic Markers in Chronic Lymphocytic Leukemia and Is Normalized by Ibrutinib Treatment. Cancers *12*, 650. https://doi.org/10.3390/cancers12030650.
42. Calissano, C., Damle, R.N., Marsilio, S., Yan, X.-J., Yancopoulos, S., Hayes, G., Emson, C., Murphy, E.J., Hellerstein, M.K., Sison, C., et al. (2011). Intraclonal Complexity in Chronic Lymphocytic Leukemia: Fractions Enriched in Recently Born/Divided and Older/Quiescent Cells. Mol. Med. *17*, 1374–1382. https://doi.org/10.2119/molmed.2011.00360.
43. Herndon, T.M., Chen, S.-S., Saba, N.S., Valdez, J., Emson, C., Gatmaitan, M., Tian, X., Hughes, T.E., Sun, C., Arthur, D.C., et al. (2017). Direct in vivo evidence for increased proliferation of CLL cells in lymph nodes compared to bone marrow and peripheral blood. Leukemia *31*, 1340–1347. https://doi.org/10.1038/leu.2017.11.
44. Jacobs, S.R., Herman, C.E., MacIver, N.J., Wofford, J.A., Wieman, H.L., Hammen, J.J., and Rathmell, J.C. (2008). Glucose Uptake Is Limiting in T Cell Activation and Requires CD28-Mediated Akt-Dependent and Independent Pathways1. J. Immunol. *180*, 4476–4486. https://doi.org/10.4049/jimmunol.180.7.4476.
45. Rathmell, J.C., Fox, C.J., Plas, D.R., Hammerman, P.S., Cinalli, R.M., and Thompson, C.B. (2003). Akt-Directed Glucose Metabolism Can Prevent Bax Conformation Change and Promote Growth Factor-Independent Survival. Mol. Cell Biol. *23*, 7315–7328. https://doi.org/10.1128/MCB.23.20.7315-7328.2003.
46. Siska, P.J., Van Der Windt, G.J.W., Kishton, R.J., Cohen, S., Eisner, W., MacIver, N.J., Kater, A.P., Weinberg, J.B., and Rathmell, J.C. (2016). Suppression of Glut1 and Glucose Metabolism by Decreased Akt/mTORC1 Signaling Drives T Cell Impairment in B Cell Leukemia. J. Immunol. *197*, 2532–2540. https://doi.org/10.4049/jimmunol.1502464.
47. Dibble, C.C., and Cantley, L.C. (2015). Regulation of mTORC1 by PI3K signaling. Trends Cell Biol. *25*, 545–555. https://doi.org/10.1016/j.tcb.2015.06.002.
48. Saxton, R.A., and Sabatini, D.M. (2017). mTOR Signaling in Growth, Metabolism, and Disease. Cell *168*, 960–976. https://doi.org/10.1016/j.cell.2017.02.004.
49. Zeng, H., and Chi, H. (2013). mTOR and lymphocyte metabolism. Curr. Opin. Immunol. *25*, 347–355. https://doi.org/10.1016/j.coi.2013.05.002.
50. Kim, J.w., Gao, P., Liu, Y.-C., Semenza, G.L., and Dang, C.V. (2007). Hypoxia-inducible factor 1 and dysregulated c-Myc cooperatively induce vascular endothelial growth factor and metabolic switches hexokinase 2 and pyruvate dehydrogenase kinase 1. Mol. Cell Biol. *27*, 7381–7393. https://doi.org/10.1128/MCB.00440-07.
51. Broecker-Preuss, M., Becher-Boveleth, N., Bockisch, A., Dührsen, U., and Müller, S. (2017). Regulation of glucose uptake in lymphoma cell lines by c-MYC- and PI3K-dependent signaling pathways and impact of glycolytic pathways on cell viability. J. Transl. Med. *15*, 158. https://doi.org/10.1186/s12967-017-1258-9.
52. Dong, Y., Tu, R., Liu, H., and Qing, G. (2020). Regulation of cancer cell metabolism: oncogenic MYC in the driver's seat. Sig Transduct Target Ther *5*, 124. https://doi.org/10.1038/s41392-020-00235-2.
53. Wilson, J.E. (2003). Isozymes of mammalian hexokinase: structure, subcellular localization and metabolic function. J. Exp. Biol. *206*, 2049–2057. https://doi.org/10.1242/jeb.00241.
54. John, S., Weiss, J.N., and Ribalet, B. (2011). Subcellular localization of hexokinases I and II directs the metabolic fate of glucose. PLoS One *6*, e17674. https://doi.org/10.1371/journal.pone.0017674.
55. Yang, T., Ren, C., Qiao, P., Han, X., Wang, L., Lv, S., Sun, Y., Liu, Z., Du, Y., and Yu, Z. (2018). PIM2-mediated phosphorylation of hexokinase 2 is critical for tumor growth and paclitaxel resistance in breast cancer. Oncogene *37*, 5997–6009. https://doi.org/10.1038/s41388-018-0386-x.
56. Ciscato, F., Filadi, R., Masgras, I., Pizzi, M., Marin, O., Damiano, N., Pizzo, P., Gori, A., Frezzato, F., Chiara, F., et al. (2020). Hexokinase 2 displacement from mitochondria-associated membranes prompts Ca^{2+} -dependent death of cancer cells. EMBO Rep. *21*, e49117. https://doi.org/10.15252/embr.201949117.
57. Tsai, S., Clemente-Casares, X., Zhou, A.C., Lei, H., Ahn, J.J., Chan, Y.T., Choi, O., Luck, H., Woo, M., Dunn, S.E., et al. (2018). Insulin Receptor-Mediated Stimulation Boosts T Cell Immunity during Inflammation and Infection.

Cell Metab. *28*, 922–934.e4. https://doi.org/10.1016/j.cmet.2018.08.003.

58. Tabatabaei Shafiei, M., Carvajal Gonczi, C.M., Rahman, M.S., East, A., François, J., and Darlington, P.J. (2014). Detecting glycogen in peripheral blood mononuclear cells with periodic acid schiff staining. J. Vis. Exp. *94*, 52199. https://doi.org/10.3791/52199.
59. Chen, D., Wang, Y., Manakkat Vijay, G.K., Fu, S., Nash, C.W., Xu, D., He, D., Salomonis, N., Singh, H., and Xu, H. (2021). Coupled analysis of transcriptome and BCR mutations reveals role of OXPHOS in affinity maturation. Nat. Immunol. *22*, 904–913. https://doi.org/10.1038/s41590-021-00936-y.
60. Sharma, R., Smolkin, R.M., Chowdhury, P., Fernandez, K.C., Kim, Y., Cols, M., Alread, W., Yen, W.-F., Hu, W., Wang, Z.-M., et al. (2023). Distinct metabolic requirements regulate B cell activation and germinal center responses. Nat. Immunol. *24*, 1358–1369. https://doi.org/10.1038/s41590-023-01540-y.
61. Brookens, S.K., Cho, S.H., Paik, Y., Meyer, K., Raybuck, A.L., Park, C., Greenwood, D.L., Rathmell, J.C., and Boothby, M.R. (2024). Plasma Cell Differentiation, Antibody Quality, and Initial Germinal Center B Cell Population Depend on Glucose Influx Rate. J. Immunol. *212*, 43–56. https://doi.org/10.4049/jimmunol.2200756.
62. Bierling, T.E.H., Gumann, A., Ottmann, S.R., Schulz, S.R., Weckwerth, L., Thomas, J., Gessner, A., Wichert, M., Kuwert, F., Rost, F., et al. (2024). GLUT1-mediated glucose import in B cells is critical for anaplerotic balance and humoral immunity. Cell Rep. *43*, 113739. https://doi.org/10.1016/j.celrep.2024.113739.
63. Rozovski, U., Hazan-Halevy, I., Barzilai, M., Keating, M.J., and Estrov, Z. (2016). Metabolism pathways in chronic lymphocytic leukemia. Leuk. Lymphoma *57*, 758–765. https://doi.org/10.3109/10428194.2015.1106533.
64. Meadows, S.A., Vega, F., Kashishian, A., Johnson, D., Diehl, V., Miller, L.L., Younes, A., and Lannutti, B.J. (2012). PI3Kdelta inhibitor, GS-1101(CAL-101), attenuates pathway signaling, induces apoptosis, and overcomes signals from the microenvironment in cellular models of Hodgkin lymphoma. Blood *119*, 1897.
65. Choi, S.-C., Titov, A.A., Abboud, G., Seay, H.R., Brusko, T.M., Roopenian, D.C., Salek-Ardakani, S., and Morel, L. (2018). Inhibition of glucose metabolism selectively targets autoreactive follicular helper T cells. Nat. Commun. *9*, 4369. https://doi.org/10.1038/s41467-018-06686-0.
66. Patra, K.C., Wang, Q., Bhaskar, P.T., Miller, L., Wang, Z., Wheaton, W., Chandel, N., Laakso, M., Muller, W.J., Allen, E.L., et al. (2013). Hexokinase 2 is required for tumor initiation and maintenance and its systemic deletion is therapeutic in mouse models of cancer. Cancer Cell *24*, 213–228. https://doi.org/10.1016/j.ccr.2013.06.014.
67. McAllister, E.J., Apgar, J.R., Leung, C.R., Rickert, R.C., and Jellusova, J. (2017). New methods to analyze B cell immune responses to the thymus dependent antigen sheep red blood cells. J. Immunol. *199*, 2998–3003. https://doi.org/10.4049/jimmunol.1700454.
68. Han, J., Gagnon, S., Eckle, T., and Borchers, C.H. (2013). Metabolomic Analysis of Key Central Carbon Metabolism Carboxylic Acids as Their 3-Nitrophenylhydrazones by UPLC/ESI-MS. Electrophoresis *34*, 2891–2900. https://doi.org/10.1002/elps.201200601.
69. Han, J., Tschernutter, V., Yang, J., Eckle, T., and Borchers, C.H. (2013). Analysis of selected sugars and sugar phosphates in mouse heart tissue by reductive amination and liquid chromatography-electrospray ionization mass spectrometry. Anal. Chem. *85*, 5965–5973. https://doi.org/10.1021/ac400769g.

STAR★METHODS

KEY RESOURCES TABLE

REAGENT or RESOURCE	SOURCE	IDENTIFIER
Antibodies		
Anti-Hexokinase-II	Abcam	Cat# epr209847
Alexa Fluor 488 goat anti-rabbit IgG	Invitrogen	Cat# A11034
BV650 anti-mouse CD138	BioLegend	Cat# 142518
BV785 anti-mouse/human B220	BioLegend	Cat# 103246
PE anti-mouse CD86	BioLegend	Cat# 105008
PE/Dazzle 594 anti-mouse IgD	BioLegend	Cat# 405742
PE/Cyanine7 anti-mouse CD95 (fas)	BioLegend	Cat# 152618
APC anti-GL7	BioLegend	Cat# 144618
Alexa Flour 700 anti-mouse CD19	BioLegend	Cat# 115528
APC/Cyanine7 anti-mouse CD3	BioLegend	Cat# 100222
APC/Cyanine7 anti-mouse/human CD11b	BioLegend	Cat# 101226
APC/Cyanine7 anti-mouse TER-119	BioLegend	Cat# 116223
APC/Cyanine7 anti-mouse F4/80	BioLegend	Cat# 123118
PE anti-mouse CD43	BioLegend	Cat# 143206
PE/Cyanine7 anti-mouse IgM	BioLegend	Cat# 406514
APC anti-mouse CD5	BioLegend	Cat# 100625
BV421 Rat anti-mouse T and B cell activation marker (GL7)	BD Biosciences	Cat# 562967
Alexa Fluor 647 F(ab)2 goat anti-rabbit IgG	Invitrogen	Cat# A21246
BV605 Anti-human CD19	BioLegend	Cat# 363024
PE anti-human CD184 (CXCR4)	BioLegend	Cat# 304504
APC anti-human CD5	BioLegend	Cat# 364016
Hamster anti-mouse CD40	BD Biosciences	Cat# 553721
Goat $F(ab')_2$ Anti-human IgM-UNLB	Southern biotech	Cat# 2022–01
Goat $F(ab)_{2\ A}$nti-mouse IgM	Jackson ImmunoResearch	Cat# 115-006-020
Chemicals, peptides, proteins		
Recombinant human sCD40L	Invitrogen	PHP0025
Recombinant human IL-4	R&D systems	204-IL/CF
Recombinant mouse IL-4	Peprotech	214-14-20UG
MitoTracker Deep Red FM	Invitrogen	M22426
Live/Dead Fixable Aqua Dead Cell Stain Kit	Invitrogen	L34966
PI3Kdelta inhibitor Idelalisib	Selleck Chemicals	S2226
pan-PI3K inhibitor Pictilisib	Selleck Chemicals	S1065
Akt inhibitor Ipatasertib	Selleck Chemicals	S2808
Akt inhibitor MK-2206	Selleck Chemicals	S1078
mTOR inhibitor rapamycin	Selleck Chemicals	S1039
mTOR inhibitor Sapanisertib	Selleck Chemicals	S2811
mTOR inhibitor JR-AB2-01	Selleck Chemicals	E1151
Glutaminase inhibitor Telaglenastat/CB-839	Selleck Chemicals	S7655
2-deoxyglucose (2DG)	Sigma-Aldrich	D3179

(*Continued on next page*)

Continued

REAGENT or RESOURCE	SOURCE	IDENTIFIER
Critical commercial assays		
Seahorse XF Glycolysis Stress Test Kit	Agilent Technologies	103020–100
Seahorse XF Real-Time ATP Rate Assay Kit	Agilent Technologies	103591–100
EasySep Mouse B cell isolation kit	Stem Cell Technologies	19854
EasySep Human B cell isolation kit	Stem Cell Technologies	100–0971
Experimental models: Cell lines		
Burkitt's lymphoma BJAB	DSMZ – German collection of microorganisms and cell cultures	ACC757
Experimental models: Organisms		
HK2-flox mice	Nissim Hay lab (Chicago, IL)	N/A
MB1-Cre (B6.C(Cg)-CD79$^{tm1(cre)Reth}$/Ehob/J	Jackson Laboratory	020505
Software and algorithms		
FlowJo	BD Biosciences	Version 10.10.0 for Mac OS
Prism	GraphPad Inc	10.2.0 for Mac OS

EXPERIMENTAL MODEL AND STUDY PARTICIPANT DETAILS

Mice

All animal experiments were approved by the University of Manitoba Animal Care Committee. HK2-flox mice were generously provided by Dr Nissim Hay (University of Illinois)[35] and crossed with MB1-Cre (Jackson Labs) to generate B cell specific deletion. Cre-negative littermates were used as HK2 wild-type controls. Genotyping and monitoring for germline deletion was done as described.[66] Mice bearing the PI3KD^{E1021K} mutation in B cells[38] were generously provided by Dr. David Rawlings (University of Washington). Mice were housed in a specific pathogen-free facility at the University of Manitoba, according to the Canadian Council on Animal Care guidelines, and used for experiments between 8 and 12 weeks of age. Both male and female mice were used for *in vitro* experiments, and no influence of sex on results was found. Female mice were used for immunization experiments.

Human samples and clinical biomarkers

Blood samples were obtained from healthy volunteers or chronic lymphocytic leukemia patients attending the CLL clinic at CancerCare Manitoba. Peripheral blood mononuclear cells were isolated using Ficoll-Paque density gradient and cryopreserved in 10% DMSO medium prior to analysis. Informed consent of patients and control subjects was obtained under a protocol approved the Research Ethics Board at the University of Manitoba. Demographic information and clinical biomarkers including ZAP70 expression were obtained from the Manitoba Tumor Bank and CAISIS database and are provided in Table S2.

Cell culture

The human B lymphoma cell line BJAB was seeded at a concentration of 5 × 10^5 cells/mL in RPMI (Hyclone Laboratories, #SH30027.01) containing 10% FBS (ThermoFisher, #12483-020) and 1% pen-strep (GE Healthcare Life Sciences, #15070-063) and incubated at 37°C and 5% CO_2. Peripheral blood mononuclear cells from healthy donors or CLL patients were isolated and cultured in the same medium at 2 × 10^6 per mL. Murine splenic B cells were isolated by negative selection using the EasySep Mouse B Cell Isolation Kit (STEMCELL Technologies, #19854A) as specified by the manufacturer's protocol. B cells were seeded at a concentration of 2 × 10^6 cells/mL in RPMI containing 10% FBS, 50μM 2-mercaptoethanol and 1% pen-strep and incubated at 37°C and 5% CO_2. Where indicated, cells were stimulated with 2 μg/mL of anti-CD40 (BD Biosciences, #553721), 10 ng/mL of IL4 (Peprotech, #214-14-20UG) and 10 μg/mL of anti-IgM (Jackson ImmunoResearch Laboratories, #115-006-020). Human B cell stimulation used 10 ng/mL Goat F(ab')$_2$ Anti-human IgM (Southern Biotech #2022-01), 2 ug/mL of recombinant human sCD40 (invitrogen PHP0025), and 10 ng/mL of recombinant human IL-4 (R&D systems, #204-IL/CF). Inhibitors used were the PI3Kdelta inhibitor Idelalisib, pan-PI3K inhibitor Pictilisib, Akt inhibitors Ipatasertib or MK-2206, mTOR inhibitors rapamycin, Sapanisertib or JR-AB2-01 or glutaminase inhibitor Telaglenastat (all from Selleck Chemicals). 2-deoxyglucose was purchased from Sigma-Aldrich (#D3179).

METHOD DETAILS

Crispr deletion of HK2

The procedure was carried out according to a protocol generously provided by Dr. Marco Cavallari from the University of Freiburg, with minor modifications. Briefly, BJAB cells were seeded at a concentration of 5 × 10^5 cells/mL in in RPMI containing 10% FBS and 1% pen-strep and

incubated at 37°C and 5% CO_2 24 h prior to the experiment. Predesigned guide RNA (crRNA:tracrRNA complex) specific for HK2 (Design ID Hs.Cas9.HK2.1.AA, sequence GGACCAACTTCCGTGTGCTTTGG) was purchased from Integrated DNA Technologies and assembled into a ribonucleoprotein complex with Cas9 according to the manufacturer's protocol (Alt-R system). BJAB cells were electroporated with the RNP complex using the Neon transfection system (ThermoFisher) as follows. Cells (1×10^6) were resuspended in 9 uL of buffer R, mixed with 1 μL RNP complex and 2 uL of 10.8 μM Alt-R Electroporation Enhancer, and electroporated at 1350 V, 40 ms, 1 pulse using a 10 uL Neon pipette tip. Cells were then transferred to 1 mL of recovery medium in a 24 well plate (RPMI+20%FCS+Glutamax+10mM HEPES). After 3 days, cells were cloned by limiting dilution and later screened by Western blotting. Approximately 50% of clones exhibited loss of HK2 protein.

RT-qPCR

Splenic B cells were stimulated as indicated and RNA was isolated using RNeasy Plus Mini Kit (Qiagen). RT-PCR was carried out as described[8] using the following primers: Fwd HK1 - CGCAGCTCCTGGCCTATTAC; Rev HK1 - GAGCCGCATGGCATAGAGAT; Fwd HK2: AGTGGAAG GCAGAGACGTTG; Rev HK2 – CAGTGCGAATGTCGTTGAGC; Fwd HK3 – TTGGGGTGCCTCATATTGCC; Rev HK3 - CTGTGCCCTTGT CACCTTGA.

Western blots

Western blots were carried out essentially as described[8] with the following modifications. SDS-PAGE was performed using 10 μg of NP-40 extract protein mixed with an equal volume of 2× Laemmli buffer (BioRad cat#: 1610737) supplemented with 5% 2-mercaptoethanol (without boiling). Mitochondrial and cytoplasmic protein was isolated using the mitochondrial/cytoplasmic fractionation kit from Millipore Sigma (cat.#: MIT1000). Primary antibodies used include the following: HK1 (Cell Signaling Technology; cat.# 2024S), HK2 (Cell Signaling Technology; cat.#: 2867S), HK3 (ThermoFisher Scientific, cat.#: PA5-84306), β-actin (Cell Signaling Technology; cat.#: 4970S), Bcl2 (Millipore Sigma; cat.#: 05-729-25UG), GAPDH (Millipore Sigma; cat.#: CS204254). Blots were visualized using the Clarity Western ECL Substrate kit (Bio Rad, cat.#: 170–5061) and imaging on a ChemiDoc MP imaging system. The relative band intensities were determined using ImageJ software.

Confocal microscopy analysis of mitochondrial localization

BJAB cells were resuspended in Dulbecco's-PBS (Gibco 14040-133) containing 10mM HEPES (Gibco 15630-106) and plated at 5×10^5 cells/mL for 2 h with the indicated stimuli/inhibitors. Cells were then stained with fixable mitochondrial dye and rabbit anti-HK2 as follows. Cells were resuspended in PBS+2% FBS buffer containing 200nM of MitoTracker Deep Red FM dye (M22426 Invitrogen) and incubated for 30 min at 37° in 5%CO2. After washing with PBS, cells were fixed with 2% paraformaldehyde, permeabilized with 0.5% saponin, stained for 3 h with a rabbit monoclonal anti-HK2 (Abcam #epr209847) at a 1:100 dilution, and finally stained with secondary AlexaFluor488-labeled goat anti-rabbit IgG (Invitrogen #A11034) at dilution of 1:200 for 30 min. Stained cells were then centrifuged onto microscope slides (Fisher #12-550-123) using a Shandon Cytospin 2 (2min x 1200 RPM) and mounted using ProLong Gold Antifade Mountant with DAPI (Thermo #P36935). Slides were imaged at 63X magnification using a Zeiss AxioObserver CSU-X1M 5000 spinning disc confocal microscope. At least 30 cells per group per experiment were imaged and Pearson's Co-Localization Coefficients were determined using the Zeiss software.

Metabolic flux assays

Extracellular acidification rate (ECAR) assays were run using a Seahorse XF24 instrument essentially as described.[8] ATP production rates were determined using the Seahorse XF Real-Time ATP Rate Assay Kit (Agilent 103591-100), according to the manufacturer's protocol. Primary mouse B cells were resuspended in the supplemented XF DMEM media to a concentration of 4×10^6 cells/mL while BJAB cells were resuspended at a concentration of 2×10^6 cells/mL and applied to assay plates coated with Poly-D-Lysine (Gibco A38904-01) or CellTak (BD Biosciences).

Flow cytometry

Peritoneal wash, spleen, bone marrow, mesenteric lymph node and Peyer's Patches were collected from 8 to 12 week old $HK2^{flox}$ x MB1-Cre+ mice, or Cre-littermate controls (with or without immunization). After preparation of single cell suspensions and washing, cells were counted and resuspended at 1×10^6/mL in FACS buffer (PBS+1% FCS) and stained for 30 min on ice with cocktails of fluorescently-labeled antibodies. In some experiments, cells were surface stained as above and then fixed, permeabilized and intracellularly stained to detect HK2. Two tubes were analyzed for every sample – one staining for HK2 as described for microscopy, and a second staining with secondary antibody alone. Cells were analyzed using a Cytoflex LX instrument equipped with 405, 488, 561 and 638nM lasers (Beckman Coulter). The resulting data were analyzed using FlowJo 10 software. For HK2 intracellular staining experiments, the mean fluorescence intensity for each population of interest was determined using both the HK2 stained and secondary-alone control tube. HK2 expression was calculated as HK2 MFI minus secondary alone background MFI for each cell population. In some experiments background subtraction was performed using population-specific background MFIs obtained from HK2 KO splenocytes stained with primary plus secondary antibody, yielding similar results.

Mouse immunization and antibody measurements

One milliliter of citrated sheep red blood cells (Colorado Serum, Denver, CO or Cedarlane Laboratories, Burlington, ON, Canada) was washed twice with 50 mL of PBS and resuspended 1:10 in PBS (0.4 mL of packed SRBCs and 3.6 mL of PBS). Two hundred microliters of

the SRBC suspension were injected intraperitoneally. Flow cytometry analyses were performed at days 4, 6 or 8 post-immunization. For antibody measurements, serum was collected on the day of immunization (day 0) and at day 5 and day10 post-immunization. Anti-SRBC Abs were measured as described.[67] Briefly, dilutions of mouse sera were incubated with washed SRBC, washed, and bound antibodies detected with anti-mouse IgM-PECy7 and anti-mouse IgG1-APC secondary antibodies. Stained SRBC were then analyzed by flow cytometry to determine mean fluorescence intensity.

In vitro B cell proliferation and antibody secretion assays

Splenic B cells were isolated by magnetic bead negative selection using EasySep mouse B cell isolation kit (Stem Cell Technology cat #19854). Cells were resuspended 2 × 10^6 cells/mL in media containing activating factors as described above and cultured at 200 uL per well in 96 well flat bottom plates for CCK8 assay or round-bottom plates for CFSE dilution and antibody secretion assays. After 3 days incubation period cell proliferation was determined using CCK8 cell viability assay, according to the manufacturer's protocol (Sigma cat#96992). Briefly, 10 uL of CCK8 reagent was added per well and after 3 h incubation the absorbance at 450 nM was measured using an ELISA plate reader. Supernatants were collected after five days of culture for antibody measurement by ELISA assay. For cell division assays, purified B cells were labeled with CFSE prior to culture, by resuspending cells at 8 × 10^6 cells per mL in PBS containing 0.6 uM CFSE, incubating for 5 min at room temperature, followed by addition of an equal volume of FBS and three washes in culture medium. At the end of the culture period cells were harvested and analyzed by flow cytometry.

Metabolite profiling

Metabolite profiling was performed through The Metabolomics Innovation Center, using the Central Carbon Metabolism assay. Briefly, metabolites were extracted from snap-frozen cell pellets using 80% methanol and sonication. TCA cycle acids, sugars and aldose phosphates were quantified by LC-MRM/MS using internal standards as described.[68,69] For other metabolites, an internal standard solution containing isotope-labeled AMP, ATP, AMP, ATP, UMP, UTP, GMP, GTP, fructose-6P, fructose-bisP, UDP-glucose, glycerol-3P, NAD, NADH and glucose-1P was prepared in 50% methanol, mixed with sample, injected into a C18 column (2.1 × 150mm, 1.7 uM) to run UPLC-MRM/MS with (−) ion detection on a Waters Acquity UPLC system coupled to a Sciex QTRAP 6500 Plus MS instrument, with the use of tributylamine acetate buffer (A) – acetonitrile-methanol (1:1) (B) as the mobile phase for gradient elution (10%–50% B over 25min) at 0.25 mL/min and 50° celcius.

^{13}C-glucose labeling and mass spectrometry

Mouse splenic B-cells were stimulated (CD40L, IL-4, F(ab')$_2$ anti-IgM) overnight at 37°C in RPMI media. The following morning the cells were washed, re-plated at 37°C in Glucose free RPMI media (Gibco, Cat. #11879020) with fresh stimulation cocktail and fully labeled D-(-+)-Glucose-^{13}C6 (Cayman Chemical Company #26707) at a final concentration of 11.1mM, and incubated for 1 h (glycolysis and pentose phosphate pathway analysis) or 4 h (TCA analysis). Following labeling, cells were washed twice with cold PBS (5 min × 300 g at 4°C) and the cell pellets were snap frozen and stored at −80°C. Analyses of stable isotope-labeled samples was performed at the Mayo Clinic Rochester mass spectrometry core facility.

QUANTIFICATION AND STATISTICAL ANALYSES

Unless otherwise indicated in figure legends, graphs present means and standard deviation (for a single representative experiment) or standard error (when pooling data from multiple independent experiments). Statistical analyses were performed using Prism software and, unless otherwise indicated, use unpaired two-tailed T-tests. Significance indicators on graphs are defined as *$p < 0.05$, **$p < 0.005$; ***$p < 0.001$), while non-significant comparisons are not marked.